LAWRENCE
LIVERMORE
NATIONAL
LABORATORY

LLNL-JRNL-832885

Low and High LET Degradation Studies of Metal-Loaded Organic Phase Ligands in the ALSEP Process

C. G. Bustillos, R. O. Ngelale, M. Nilsson

March 16, 2022

Solvent Extraction and Ion Exchange

Disclaimer

Low and High LET Degradation Studies of Metal-Loaded Organic Phase Ligands in the ALSEP Process

Christian G. Bustillos[a,*], Randy O. Ngelale[b], Mikael Nilsson[c]

[a]Lawrence Livermore National Laboratory, Livermore, CA, USA; [b]Oak Ridge National Laboratory, Oak Ridge, TN, USA; [c] formerly: University of California, Irvine, Irvine, CA, USA

*Corresponding Author: bustillos2@llnl.gov

Abstract

Organic solutions comprising the Actinide Lanthanide Separation Process (ALSEP) solvent consisting of 0.5 M 2-ethylhexyl phosphonic acid mono-2-ethylhexyl ester (HEH[EHP]) and 0.05 M N,N,N',N'-tetra(2-ethylhexyl)diglycolamide (T2EHDGA) in *n*-dodecane were subjected to low LET and high LET irradiation before and after equilibration with an aqueous phase of 3 M HNO_3. Degradation dose constants revealed greater ligand degradation due to gamma irradiation than alpha irradiation for both ligands. Furthermore, equilibration with nitric acid did not have a significant impact on ligand degradation for either irradiation source. Identified degradation products were similar for both gamma and alpha irradiation and occurred mostly through the rupture of the N–$C_{carbonyl}$ and C–O_{ether} bonds for T2EHDGA and the C–O_{ether} bond in HEH[EHP]. Acid contact appears to alter the degradation pathway by favoring the formation of higher molecular weight recombination products. Mixed T2EHDGA-HEH[EHP]-NO_3 complexes were formed with Nd(III) after extraction from 3 M HNO_3, and low LET gamma irradiation of the Nd(III) loaded organic solution produced similar degradation products as the organic solution absent of Nd(III). Interestingly, and likely due to the greater radiolytic susceptibility of T2EHDGA than HEH[EHP], a HEH[EHP]-Nd(III) complex appears to form with increasing absorbed dose.

Introduction

Closing of the nuclear fuel cycle relies on some concept of partitioning of elements in the used nuclear fuel followed by reuse of the fissile material in a mixed oxide fuel. In cases where long-lived waste is targeted for removal, transmutation, i.e. the conversion of highly radiotoxic elements to short-lived nuclides, follow the partitioning. Thus, continued research in advanced separation

processes is imperative for driving support and implementation towards this goal.[1] The successful separation and transmutation of long-lived radiotoxic nuclides to short-lived nuclides is expected to minimize heat load concerns from radioactive decay during long-term storage in a geological repository and ease volume storage constraints.[2] The removal of uranium and plutonium from used nuclear fuel (UNF) has been practiced commercially for decades through the Plutonium Uranium Reduction Extraction (PUREX) Process utilizing liquid-liquid extraction, exploiting the unique redox chemistry of those elements.[3–5] However, the long-lived and highly radiotoxic transuranium elements americium (Am) and curium (Cm) are not efficiently extracted in this process. The isolated recovery of Am and Cm (trivalent actinides, An(III)) is rendered difficult due to their aqueous solution chemistry having strong chemical and physical similarity to that of trivalent lanthanides (Ln(III)).[6] Selective partitioning of the An(III) elements from Ln(III) is imperative as Ln(III) are abundant in UNF, and would have a detrimental impact on the transmutation process.[7] Several solvent extraction efforts have been developed and proposed addressing An(III)/Ln(III), although none are yet practiced commercially.[8–11] Several of these processes rely on the co-extraction of An(III) and Ln(III) after the removal of U and Pu through a PUREX step, followed by the selective stripping of An(III) into an aqueous phase.[12] Current international UNF reprocessing efforts, such as the current EURO-GANEX (Group Actinide Extraction) rather focus on the group extraction of the actinides, including U and Pu, and utilize a combination of co-extracting amides in order to achieve desired separation goals.[13–15] The Actinide Lanthanide Separation (ALSEP) Process has been developed for efficient An(III)/Ln(III) separation, with the inherent benefit of An(III)/Ln(III) extraction from a wide range of highly acidic aqueous solutions, less sensitivity to changes in pH during An(III) stripping, faster extraction rates, and less affinity for fission products.[16, 17] The ability to extract from highly acidic aqueous solutions allow for An(III)/Ln(III) extraction immediately after a PUREX step, simplifying flowsheet complexity and minimizing waste. The benefits employed by the ALSEP Process are driven by incorporating an organic diluent comprised of the combination of a neutral diglycolamide and an acidic dialkylorganophosphorus compound, each of which have been heavily employed in hydrometallurgical processes.[18–24] The neutral diglycolamide extractant is expected to predominantly partake in An(III)/Ln(III) extraction from acidic aqueous solutions (3 M HNO_3), while the acidic dialkylorganophosphorus extractant retains Ln(III) while An(III) is stripped into an aqueous buffer at pH = 2 – 4. Through thorough investigation and iteration, the

combination of 0.05 M N,N,N',N'-tetra(2-ethylhexyl)diglycolamide (T2EHDGA) and 0.5 M 2-ethylhexyl phosphonic acid mono-2-ethylhexyl ester (HEH[EHP]) in *n*-dodecane have been deemed the most effective organic solvent (Figure 1).

Due to the inherent radioactive nature of UNF, liquid-liquid separation systems must be resistant to ionizing radiation as extracting agents will be subjected to gamma and alpha induced degradation. The ALSEP extractants are intended for Am and Cm partitioning, therefore T2EHDGA and HEH[EHP] will be exposed to a relatively high intensity of alpha particles.[25, 26] The radiolytic gamma degradation of T2EHDGA, HEH[EHP], their combination, and the effect on extraction efficiency has been well documented.[27–33] Low LET gamma irradiation of the ALSEP solvent decreased Am (D_{Am}) extraction by an order of magnitude after an absorbed dose of 800 kGy which was attributed to the radiolytic degradation of T2EHDGA.[33] Although the effect of low LET gamma radiation on T2EHDGA, and on alkyldiglycolamides in general, has been extensively[31, 33–36] To date, investigations on the effect of high LET, i.e. alpha, radiation on the constituents of the ALSEP extractant system is limited.[37, 38] It has also been previously reported that the presence of impurities, particularly phosphonic acids formed from HEH[EHP] degradation, in the extracting organic solvent leads to an increase in the retention of Am(III) (high D_{Am} values) in the organic phase during a stripping phase, contributing to inefficient An(III)/Ln(III) separation.[33, 39] Although the degradation products of T2EHDGA by gamma radiolysis have been reported[31], the effect of the presence of HEH[EHP] on the degradation pathway has not been investigated. Due to the nature of high LET alpha particles, which deposit their energy in short distances, degradation products from alpha radiolysis must also be investigated. Additionally studies on the effect of incident radiation on metal-ligand complexes are also limited.[40, 41]

Aims and Scope

In this work, an ALSEP organic solution equilibrated with Nd(III), a surrogate for Am(III) owing to similar ionic radii, at extracting conditions (3 M HNO_3) underwent low LET gamma irradiation followed by degradation product analysis.[42] Identification of radiolytic degradation products relied on the utilization of ESI-MS, which can preserve and transport the metal ligand complexes from solution to gas phase, acquiring structural information about the complexes in solution.[43, 44] Structures identified through ESI-MS results can provide information on the potential impact on

the separation process, in particular regarding the stripping phase. Irradiated solutions were also analyzed by absorption and vibrational spectroscopy which provided valuable insights. In addition to studying metal loaded systems, high LET irradiation of organic solutions before and after contact with a representative aqueous solution, albeit without extractable metals, were also undertaken. The high LET irradiations employed a method by which an alpha particle is produced in situ, via the $^{10}B(n,\alpha)^{7}Li$ reaction. Previous work from our laboratory have shown that this method provides high LET degradation that is comparable to the alpha radiation from transuranic actinides.[41, 45–47]

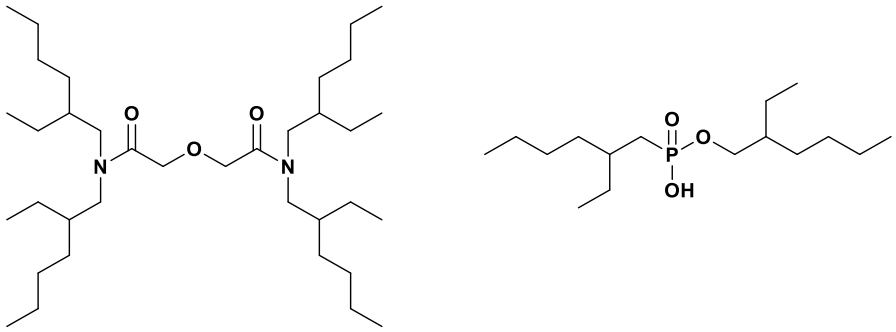

Figure 1. Structural representations of N,N,N',N'-tetra(2-ethylhexyl)diglycolamide (T2EHDGA, Left) and 2-ethylhexyl phosphonic acid mono-2-ethylhexyl ester (HEH[EHP], right)

Experimental

Materials and Samples Preparation

N,N,N',N'-tetra(2-ethylhexyl)diglycolamide (T2EHDGA, 97+%) and 2-ethylhexylphosphonic acid mono-2-ethyhexyl ester (HEH[EHP], min. 98%) were acquired from Marshallton Research Laboratories (King, North Carolina, USA) and utilized without additional purification. Neodymium solutions were prepared from neodymium nitrate hexahydrate (99.9%, Alfa Aesar). An ALSEP solution consisting of 0.5 M HEH[EHP] and 0.05 M T2EHDGA was prepared by dissolving appropriate amount of ligand in *n*-dodecane (99%, Alfa Aesar, Havervill, Massachusetts, USA). Aqueous solutions were prepared and diluted in ultra-pure water (MilliQ, 18 MΩ). Neodymium solutions of 0.5, 0.1, 0.05, 0.01, and 0.001 M Nd^{3+} were prepared in 3 M

HNO_3 (Macron, Randor, Pennsylvania, USA). Aliquots of 10 mL of organic and aqueous phases were equilibrated in borosilicate glass vials (QorPak, Clinton, Pennsylvania, USA) for 15 minutes and centrifuged. After phase disengagement and separation, the organic phases were collected for high and low LET irradiations. The organic solutions intended for high LET irradiation incorporated bis(pinacolato) diboron (99%, Sigma Aldrich, St. Louis, Missouri, USA) for a final boron concentration of 0.4 M.

Low LET Gamma Irradiations

A Cs-137 source (Cs137 Irradiator Mark-I, Model 68, JL Shepherd & Associates, San Fernando, California, USA) with 661 keV gamma rays was utilized for low LET irradiations. The source was calibrated for dose to water by Fricke dosimetry before the start of irradiation of the organic solutions.[48] The dose rate determined at the position of organic solutions during irradiation was determined to be 2.14 ± 0.06 kGy/h. The organic solutions in sealed glass vials were irradiated for 15 days for a total absorbed dose of 771 kGy. At different time intervals, the organic solutions were removed from the gamma irradiator cell and 500 μL of each organic solution was removed for gas chromatography, mass spectrometry, FT-IR, and absorption spectroscopy. The organic solutions were then immediately placed back in the gamma irradiator cell after sampling. Although oxygen is introduced back into organic solution during sampling, it is presumed that any introduced oxygen is consumed rapidly once the solution is back in the gamma irradiator cell and the effect of oxygen in the irradiated solutions is negligible.[41]

High LET Irradiations

Organic solutions were irradiated at the UC Irvine TRIGA® reactor (General Atomics, San Diego, California, USA) where they were exposed to a mix of high and low LET radiation. Details of the incorporation of boron containing compounds for high LET studies has been discussed in previous studies.[41, 45–47, 49] The low LET dose rate from the reactor core has been determined to be 40.1 kGy/h during operation at steady operation at 250 kW and represents the gamma emissions from fission products as well as the ambient effects of neutron activation within the samples followed by subsequent gamma decay. The organic solutions were irradiated up to 6.8 h at 250 kW reactor power in the rotating Lazy Susan rotary rack. The samples receive a thermal neutron flux of 8 x 10^{11} neutrons/cm^2/s which translates, using 0.4 M boron, to an approximate high LET dose of 211 kGy/h due to ^{4}He and ^{7}Li recoils from the ^{10}B(n,α)^{7}Li reaction. Irradiation times were chosen in

order to achieve a total dose comparable to the low LET gamma irradiation in the Cs-137 irradiator cell. Organic solutions without Boron were also irradiated simultaneously in the Lazy Susan rotary rack to account for the background dose.

Gas Chromatography

A Hewlett-Packard 5890 Gas Chromatograph using a flame-ionization detector, equipped with a 30-m DB 5ms column (Agilent Technologies, Santa Clara, California, USA), and an associated Hewlett-Packard Controller 7673 A integrator was utilized to determine the concentration of HEH[EHP] and T2EHDGA after irradiation. Irradiated samples were diluted 1:150 in hexane, and triphenyl phosphate was added to each diluted sample to function as an internal standard to monitor the performance and consistency of the GC. A derivatization agent, diazomethane, was also added to each diluted solution in order to add a methyl group to acidic compounds which could be retained by silica within the GC column. Diazomethane was prepared within a diazomethane generator kit (Sigma Aldrich) using diazald (99%, Sigma Aldrich), Carbitol (99%, Sigma-Aldrich), and potassium hydroxide (Fischer Scientific).

Mass Spectrometry, Infrared, and Absorption Spectroscopy

Samples of irradiated solution were diluted 1:1000 in HPLC grade 2-propanol and were analyzed by mass spectrometry using a Waters Micromass LCT 3 running a 20 μL injection at 0.1 mL/min in 100% MeOH in positive and negative mode analysis. IR measurements were recorded on a Jasco FTIR-4700 – ATR PRO ONE equipped with ATR-PRO ONE crystal. All spectra were collected between 400 – 4000 cm^{-1} using 32 scans and a resolution of 4 cm^{-1}. Absorption spectra were recorded on an Olis upgraded Cary-14 UV/Vis/NIR spectrophotometer scanning in the 500 – 900 nm at a resolution of 0.5 nm.

Results and Discussion

Low LET Degradation Constants of HEH[EHP] and T2EHDGA

The gamma induced degradation of T2EHDGA in *n*-dodecane (Figure 2b) appeared to follow an exponential degradation trend. Changes in ligand concentration after exposure to irradiation which follow an exponential decay function have been treated analogously to pseudo first-order kinetics,

as also observed during the radiolysis of TODGA[31, 50], and the radiolytic degradation as a function of dose is referred to as the dose constant.[51] The radiolytic degradation dose constant for T2EHDGA for low LET (k_γ) was determined from the value of the exponential constant:

$$\frac{d[L]}{dDose} = -k_\gamma[L] \quad (eq.\,1)$$

$$[L] = [L]_0 e^{-(k_\gamma)Dose} \quad (eq.\,2)$$

Equation 2 represents the basis of the degradation model used to characterize the degradation profile for low LET gamma radiation where [L] represents ligand concentration. HEH[EHP] does not appear to exhibit the characteristic exponential consumption pattern indicative of first or pseudo first order kinetics but rather appears to proceed linearly with absorbed dose (Figure 2a). This suggests pseudo zero order kinetics as the reaction proceeds seemingly independent of the abundance of the ligand, and a multi-step degradation mechanism as reported for the radiolysis of CMPO is likely.[50, 52–54] There is also a likely a slower rate limiting step that must occur between the HEH[EHP] ligand molecule and radical cation species that does not depend on the concentration of the ligand. HEH[EHP] is therefore modeled using pseudo zero order kinetics:

$$\frac{d[L]}{dDose} = -k_\gamma \quad (eq.\,3)$$

$$[L] = [L]_0 - k_\gamma\,Dose \quad (eq.\,4)$$

Figure 2a and 2b shows the fit between our experimentally determined concentration profiles after irradiation and the degradation model for HEH[EHP] and T2EHDGA respectively. During low LET gamma irradiation of the ALSEP solvent, T2EHDGA undergoes radiolytic degradation at a faster rate than HEH[EHP]. Low LET gamma degradation constants were determined to be (3.23 ± 0.28)×10^{-3} kGy^{-1} for T2EHDGA and (2.32 ± 0.29)×10^{-4} $mol{\cdot}L^{-1}{\cdot}kGy^{-1}$ for HEH[EHP]. The degradation dose constant for T2EHDGA differs significantly from the degradation dose constant of T2EHDGA (1.6 ± 0.04)x10^{-3} kGy^{-1} in a solution consisting of 0.05 M T2EHDGA + 0.75 M HEH[EHP] in *n*-dodecane irradiated in an irradiation test loop at Idaho National Laboratory by Peterman et al.[33] While much higher than the value reported by Peterman et al., those reported here are slightly lower than the degradation dose constant corresponding to 0.05 M TODGA (4.1 ± 0.3)x10^{-3} kGy^{-1} and 0.05 M T2EHDGA ± 0.3)x10^{-3} kGy^{-1} in *n*-dodecane from studies by Zarzana

et al.[31] Our degradation dose constants are also compared (Table 1) to that of three separate 0.05 M methylated TODGA derivatives in *n*-dodecane (2.9, 3.0 and 5.0×10^{-3} kGy^{-1}) and 0.05 M dioctyl and didodecyl substituted alkyldiglycolamides $(4.1 \pm 0.3) \times10^{-3}$ kGy^{-1}.[35, 55, 56]

Degradation dose constants after pre-equilibration with 3 M HNO_3 were determined as $(2.45 \pm 0.33)\times10^{-3}$ kGy^{-1} for T2EHDGA and $(2.00 \pm 0.34)\times10^{-3}$ $mol\cdot L^{-1}\cdot kGy^{-1}$ for HEH[EHP] (Table 2). Determined degradation dose constants are comparable to those corresponding to not pre-equilibrated with nitric acid suggesting the presence of nitric acid does not play a significant protective role, consistent with studies reporting that pre-equilibration with an acidic aqueous phase did not significantly alter the radiolytic degradation rate of diglycolamides.[31, 33–35, 56]

Table 1. Measured gamma degradation dose constants for T2EHDGA irradiated in Cs-137 gamma irradiator cell and comparisons to reported literature values.

	Dose constant k_γ (kGy^{-1} or $mol\cdot L^{-1}\cdot kGy^{-1}$)
0.05 M T2EHDGA (this work)	$(3.23 \pm 0.28)\times10^{-3}$
0.05 M T2EHDGA + 3 M HNO_3 (this work)	$(2.45 \pm 0.33)\times10^{-3}$
0.05 M T2EHDGA[33]	$(1.6 \pm 0.04)\times10^{-3}$
0.05 M TODGA[31]	$(4.1 \pm 0.3)\times10^{-3}$
0.05 M T2EHDGA[31]	$(4.3 \pm 0.3)\times10^{-3}$
0.05 M MeTODGA[55]	$(5.0 \pm 0.3)\times10^{-3}$
0.05 M Me_2TODGA[55]	$(3.0 \pm 0.2)\times10^{-3}$
0.05 M D^3DODGA[56]	$(4.1 \pm 0.3)\times10^{-3}$
0.05 M mTDDGA[35]	$(2.9 \pm 0.1)\times10^{-3}$

The radiation effects on the organic phase ligands discussed here are likely due primarily to indirect radiolysis by radical species generated by direct radiolysis. N-dodecane comprises a significant proportion of the system and presents the bulk of electrons available to interact with incident ionizing radiation. The radiation effects on the organic phase ligands are likely due to indirect radiolysis by radical species generated by direct radiolysis. N-dodecane comprises a significant proportion of the organic solvent system and presents the bulk of electrons available to interact with incident ionizing radiation. The radiolytic degradation of alkanes, including *n*-

dodecane, during biphasic solvent extraction can be generally expressed by the non-stoichiometric reaction[36, 53, 57, 58] (eq. 5):

$$CH_3(CH_2)_nCH_3 \rightarrow e^-_{sol} + {}^{\bullet}[CH_3(CH_2)_nCH_3]^+ + {}^{\bullet}CH_2(CH_2)_nCH_3 + {}^{\bullet}CH_3 + {}^{\bullet}H + H_2 \quad \text{(eq. 5)}$$

During exposure to the aerated aqueous phase, the radicals e^-_{sol}, ${}^{\bullet}CH_3(CH_2)_nCH_3$, ${}^{\bullet}CH_3$, and ${}^{\bullet}H$ will (be consumed) react with dissolved oxygen and the solvent radical cation ${}^{\bullet}(CH_3(CH_2)_nCH_3]^+$ will be the predominant contributor to ligand degradation.[36] However, degradation dose constants suggest radicals formed after contact with an aqueous phase do not play a significant role in the ligand degradation. Absent of an aerated aqueous phase, radiolytic degradation of the alkane diluent will produce solvated electrons and the radical cation[53] (eq. 6):

$$CH_3(CH_2)_nCH_3 \rightarrow e^-_{sol} + {}^{\bullet}[CH_3(CH_2)_nCH_3]^+ \quad \text{(eq. 6)}$$

The radiolytic products of *n*-dodecane (eq. 6) can undergo reductive electron transfer (eq. 7), oxidative electron transfer (eq. 8) or proton transfer (eq. 9) with the dissolved ligands[36, 59]:

$$e^-_{sol} + L \rightarrow {}^{\bullet}[L] \quad \text{(eq. 7)}$$

$${}^{\bullet}[C_{12}H_{26}]^+ + L \rightarrow C_{12}H_{26} + {}^{\bullet}[L]^+ \quad \text{(eq. 8)}$$

$${}^{\bullet}[C_{12}H_{26}]^+ + L \rightarrow C_{12}H^{\bullet}_{25} + {}^{\bullet}[LH^+] \quad \text{(eq. 9)}$$

The solvated electron (e^-_{sol}) will mostly react with the solvent rather than the ligand and is not expected to play a significant role in ligand radiolysis despite being a reducing agent.[60] The production of the *n*-dodecane radical during irradiation (${}^{\bullet}[C_{12}H_{26}]^+$) will react with the ligands with fast reaction kinetics and will predominantly contribute to ligand degradation.[31, 36, 50, 52, 58, 61] Due to the first order kinetics of T2EHDGA degradation, the dodecane radical cation charge transfer occurs directly with T2EHDGA, and due to the zero order degradation, through an intermediate or multi-step reaction with HEH[EHP].[31, 58] Radiolytic degradation of T2EHDGA and HEH[EHP] of the ALSEP solvent is therefore expected to occur through electron or proton transfer induced by the *n*-dodecane radical, and all discussion of ligand degradation will presume radiolysis generally occurs through this charge transfer.

High LET Degradation Constants of T2EHDGA and HEH[EHP]

A method similar to the low LET scenario was utilized to determine the high LET degradation constants. However, due to the reactor core consisting of a mixed radiation field, equations 2 and 4 are modified to account for both the high and low LET contributions to the degradation of the ligands. Equations 10 and 11 assume that high and low LET impacts are additive[43] in order to relate the concentration of ligand (L) to the high and low LET dose rates, $\dot{D}_\alpha$ and $\dot{D}_\gamma$, respectively. Similarly, t_α and t_γ represent the irradiation times while k_α and k_γ are the degradation constants for high and low LET, respectively. Owing to the inability to exclusively obtain high LET experimental data, the changes in ligand concentration (Figure 2) due to high LET irradiation was estimated by equations 10 and 11.

$$[L] = [L]_0 e^{-(k_\alpha \dot{D}_\alpha t_\alpha + k_\gamma \dot{D}_\gamma t_\gamma)} \quad \text{(eq. 10)}$$

$$[L] = [L]_o - (k_\alpha \dot{D}_\alpha t_\alpha + k_\gamma \dot{D}_\gamma t_\gamma) \quad \text{(eq. 11)}$$

Since the initial, transient (at the time of sampling), and final ligand concentrations are known, the irradiation times are recorded, and the dose rates have been previously determined, the only unknowns in equation 10 and 11 are the dose constants. Utilizing the previously determined low LET gamma irradiation dose constant, equations 10 and 11 become solvable. In order to ensure consistency, samples containing no boron were irradiated with the assumption that the degradation profile for both HEH[EHP] and T2EHDGA by the background gamma rays and neutrons matches the low LET profile determined from the Cs-137 irradiator cell. Figure S1 in the ESI shows the good agreement in low LET gamma irradiation between the Cs-137 gamma irradiator cell and the reactor core low LET dose. Calculated degradation dose constants reveal T2EHDGA undergoes greater degradation than HEH[EHP] in the presence of alpha particles, but both ligands undergo significant more degradation when exposed to gamma radiation (Table 2, Figure 2). Note that in the reactor core, the dose rates were 40 kGy/h for the background low LET gamma and 211 kGy/h for the high LET alpha radiation. The apparent lower degradation of the ligands in the combined dose, reactor core irradiations, is due to the much lower degradation constant for high LET irradiation. As observed with low LET gamma irradiations, there is no significant difference in alpha degradation dose constant of HEH[EHP] or T2EHDGA after pre-equilibration with 3 M HNO_3. Determine degradation dose constants for alpha and gamma irradiation are consistent with previous studies reporting more severe degradation for low LET irradiation than high LET

irradiation for other ligands utilized in f-element extractive separations such as TBP, CMPO, $CyMe_4$-BTBP, DMDOHEMA, and DTPA.[41, 47, 52, 62–65]

Table 2. Comparison of measured gamma and alpha degradation constants dose constants for HEH[EHP] and T2EHDGA.

	Dose constants (kGy^{-1} or $mol \cdot L^{-1} \cdot kGy^{-1}$)	
	High LET k_α	Low LET k_γ
0.5 M HEH[EHP]	$(1.77 \pm 0.22) \times 10^{-4}$	$(2.32 \pm 0.29) \times 10^{-4}$
0.5 M HEH[EHP] + 3 M HNO_3	$(1.64 \pm 0.16) \times 10^{-4}$	$(2.00 \pm 0.34) \times 10^{-4}$
0.05 M T2EHDGA	$(1.03 \pm 0.13) \times 10^{-3}$	$(3.23 \pm 0.28) \times 10^{-3}$
0.05 M T2EHDGA + 3 M HNO_3	$(9.45 \pm 0.39) \times 10^{-4}$	$(2.45 \pm 0.33) \times 10^{-3}$

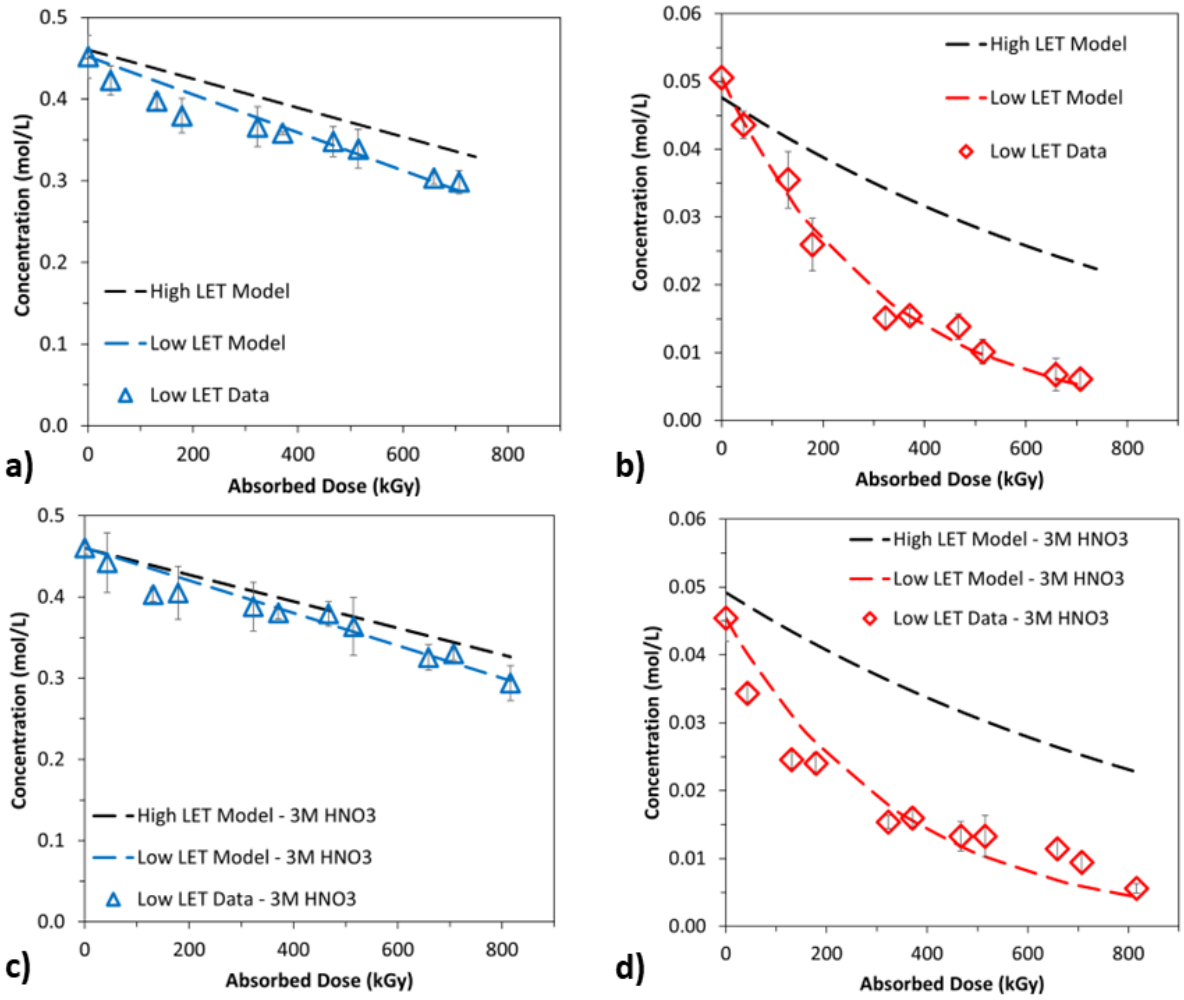

Figure 2. Concentration as a function of dose for low LET (Cs-137 Gamma Irradiator Cell) as well as model predicted high LET irradiation dose (reactor irradiation) for a) 0.5 M HEH[EHP] b) 0.05 M T2EHDGA c) 0.5 M HEH[EHP] + 3 M HNO_3 and d) T2EHDGA + 3 M HNO_3. Dose rates were 2.14 kGy/h in the Cs-137 Gamma Irradiator Cell and 211 kGy/h (high LET) in the reactor core.

The apparent differences in responses elicited by low and high LET radiation lend further weight to the idea that the dominant pathway of radiolysis in the system discussed is indirect radiolysis. Due to their larger sizes, charged particles such as the alpha particle deposit their energy in more condensed tracks. These tracks may be viewed as reaction volumes in which the radical species produced by the particle are more likely, due to their proximity with one another within the volume, to undergo recombination with each other to form molecular species prior to reacting with the

ligands.[57] The radiolytic products in eq. 5 should be present in higher yields after high LET exposure in comparison to low LET.[66] Low LET gamma rays deposit their energies along longer more spurious tracks. In geometric terms, as track length increases and track width decreases, the surface area over which reactions between radical species inside the volume can react with molecular species outside of it increases while the volume for radical recombination decreases. The rapid recombination of radical species also results in slower degradation of TODGA and CMPO.[38, 52]

Absorption Spectroscopy of Low LET Irradiation of Nd(III) Loaded ALSEP

Absorption spectroscopy was utilized to probe the metal cation environment in the organic phase after irradiation of the metal loaded organic solution. The absorption spectrum of Nd(III) in 3 M HNO_3 is characterized by absorption bands at 500 – 540 nm ($^4I_{9/2} \rightarrow {}^4G_{9/2}$, $^4G_{7/2}$, $^2K_{13/2}$), 670 – 700 nm ($^4I_{9/2} \rightarrow {}^4F_{9/2}$), and a broad peak centered at 579 nm (Figure S2).[67, 68] The hypersensitive behavior of the transition of the Nd(III) cation between 560 – 600 nm ($^4I_{9/2} \rightarrow {}^4G_{5/2}$, $^2G_{7/2}$) can elucidate the nature of the local coordination environment of the extracted species, and therefore changes in coordination of the species with increase in absorbed dose.[67, 69–72] The absorption spectrum of the ALSEP solvent contacted with 0.5 M Nd(III) is characterized by transitions at 576 and 584 nm (Figure 3) while the solutions contacted with 0.1 and 0.05 M Nd(III) include a shoulder at 587 nm (Figure S3). The absorption spectra are generally consistent with previous studies reporting the absorption spectra of the ALSEP solvent equilibrated with Nd(III) in 3 M HNO_3.[73, 74] The transitions corresponding to extracted Nd(III) in the ALSEP solvent generally decrease in intensity and broaden with increasing absorbed dose (Figure 3). However, at 720 kGy for equilibration with 0.5 M and 0.1 M Nd(III), and at 672 kGy, and above, for equilibration with 0.05 M Nd(III), the absorption intensity increases. After an absorbed dose of 720 kGy, sharp transitions at 572 and 592 nm appear giving the spectra of the irradiated solvent 4 distinct transitions (Figure 3). The intensity of the transitions at 572 nm appears to increase after an absorbed dose of 96 kGy. Most notably, there is an isobestic point at 574 nm which suggests the presence of multiple absorbing Nd(III) species. Studies by Muller at al. also observed multiple isosbestic points, including one at 572 nm, as a diamide was titrated into a solution comprised of Nd(III)-HDEHP.[75] The transition at 574 nm is also characteristic of and bears a strong resemblance to the absorption

spectra of Nd(III) equilibrated HEH[EHP] and HDEHP.[73–76] Therefore, it is likely the absorption spectrum after an absorbed dose of 720 kGy could correspond to the predominance of the $Nd((HEH[EHP])_2)_3$ complex. In general, the absorption intensity of the hypersensitive Nd(III) band at 584 nm tends to increase with both increasing number of coordinated ligands and decrease in their metal-ligand bond length.[77] The decrease in intensity with absorbed dose could be attributed to the dissociation of both T2EHDGA and nitrates from Nd(III) due to their radiolytic degradation. The association of HEH[EHP] with Nd(III), resulting in an increasing absorbance intensity at the highest doses, particularly at 572 nm, could be enhanced due to the radiolytic susceptibility of T2EHDGA compared to HEH[EHP] and the greater initial HEH[EHP] concentration (0.5 M).

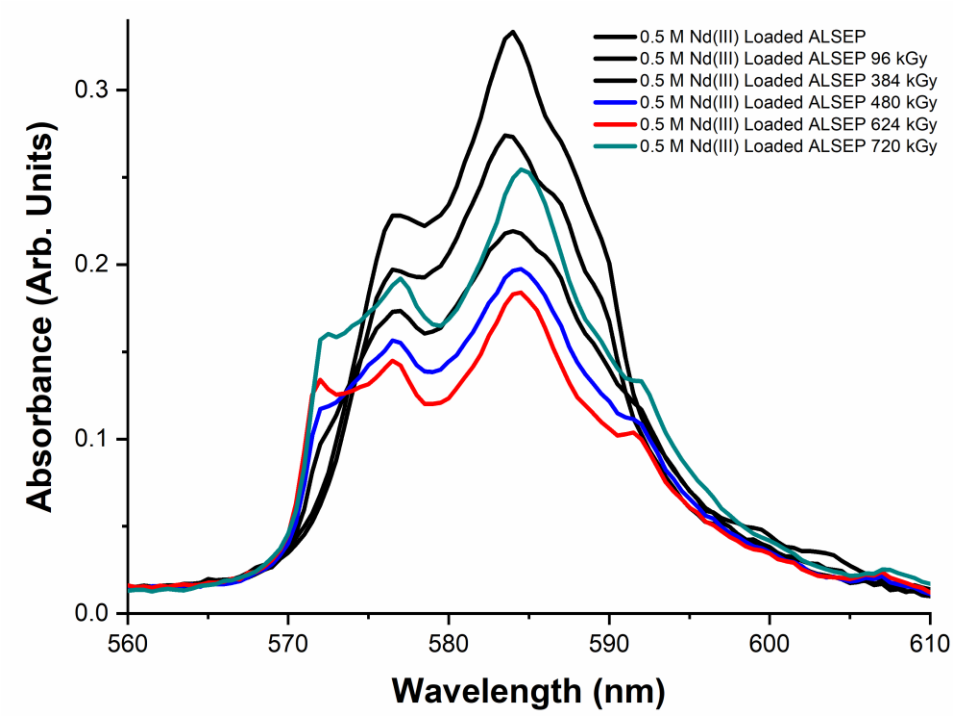

Figure 3. Absorption spectra of gamma irradiation of 0.5 M HEH[EHP] + 0.05 M T2EHDGA organic solution equilibrated with 0.5 M Nd(III) in 3 M HNO_3.

Vibrational Spectroscopy of Low LET Irradiated ALSEP

FT-IR spectroscopy was utilized to further probe ligand interactions and environment between the T2EHDGA and HEH[EHP] before and after low LET gamma irradiation of the:

- ALSEP solvent (Figure S4)
- ALSEP solvent after pre-equilibration with 3 M HNO_3 (Figure 4, S5)
- ALSEP solvent after contact with Nd(III) in 3 M HNO_3 (Figure 5, S6, S7)

The FT-IR spectra of the ALSEP solvent generally resembles the spectra of organic solvent mixtures comprised of amide containing compounds and alkyl phosphoric or alkyl phosphonic acids (Figure S4).[71, 74, 78–80] The FT-IR spectra of the HEH[EHP] and T2EHDGA solution is characterized by transmittance peaks at 1655 – 1664 cm^{-1} and 1118 cm^{-1}, corresponding to amide C=O and ether C–O stretching frequencies of the T2EHDGA ligand, and peaks at 1198 cm^{-1}, doublet at 1038 cm^{-1}, 1026 cm^{-1}, and 981 cm^{-1} corresponding to phosphoryl P=O, P–O–C, and P–OH stretching of the HEH[EHP] ligand, respectively (Figure S4, Table 3).[71, 74, 76, 78] Additionally, the splitting of the P–O–C stretches at 1026 and 1038 cm^{-1} is likely attributed to stereoisomers around the stereogenic P atom.[76] After an absorbed dose of 720 kGy, there is an overall intensity weakening of the transmittance peaks, primarily in the amide C=O and ether C–O stretching frequencies of the T2EHDGA ligand, suggesting ligand degradation through N–$C_{carbonyl}$ and $C_{methylene}$–O_{ether} bond rupturing. Although present in relatively low intensity, additional peaks are observed in the range of 1672 – 1720 cm^{-1} after irradiation which could be attributed to the formation and presence of additional carbonyl C=O containing groups arising from the degradation of T2EHDGA,[34] and vibrational frequencies attributed to carboxylic acids and amides formed from the radiolysis of branched alkylamides are typically observed at 1730 cm^{-1} and 1630 cm^{-1} respectively.[61, 81–83] The additional presence of a low intensity shoulder at 1102 cm^{-1}, corresponding to a C–N stretch in an aliphatic amine, further suggests rupturing of the N–$C_{carbonyl}$ bond in the T2EHDGA ligand[84], and the slight intensity decrease of the P–O–C stretching frequency of the HEH[EHP] ligand could correspond to rupturing of the $C_{methylene}$–O_{ether} bond.

The spectra of the ALSEP solvent pre-equilibrated with 3 M HNO_3 (Figure 4, S5) is primarily characterized by a significant broadening in the region 1560 – 1710 cm^{-1} attributed to the overlap between amide carbonyl C=O stretch and bonded carbonyl and nitrate C=O–HNO_3 due to the extraction of nitric acid,[29, 85] and a shoulder at 1293 cm^{-1} is also indicative of the presence of nitric acid coordinated HEH[EHP] in the organic solution.[80, 84, 86] After an absorbed dose of 816 kGy,

there is a weakening in the intensity of the bands corresponding to the T2EHDGA carbonyl amide C=O at 1655 cm^{-1} and ether C–O 1120 cm^{-1} stretching frequencies (Figure 4). A prominent peak at 1718 cm^{-1} likely corresponds to the presence of carbonyl and aliphatic amine groups containing compounds arising from the rupturing of T2EHDGA at the amide N–$C_{carbonyl}$ position. The peak at 1718 cm^{-1} is more pronounced and significantly more intense than observed in the spectra of the irradiated non-acid pre-equilibrated ALSEP solvent (Figure S4), suggesting a possible altered degradation pathway during irradiation in the presence of nitric acid, consistent with IR analysis reporting evidence of competing radiolytic degradation mechanisms for alkyl amides irradiated in the presence and absence of nitric acid.[61, 84] There is also an overall decrease in the broadening of the band at 1655 cm^{-1} and a decrease in the transmittance of the shoulder at 1280 cm^{-1}, consistent with a decrease in nitric acid in an organic phase after irradiation due to the radiolysis of extracted HNO_3.[61, 84]

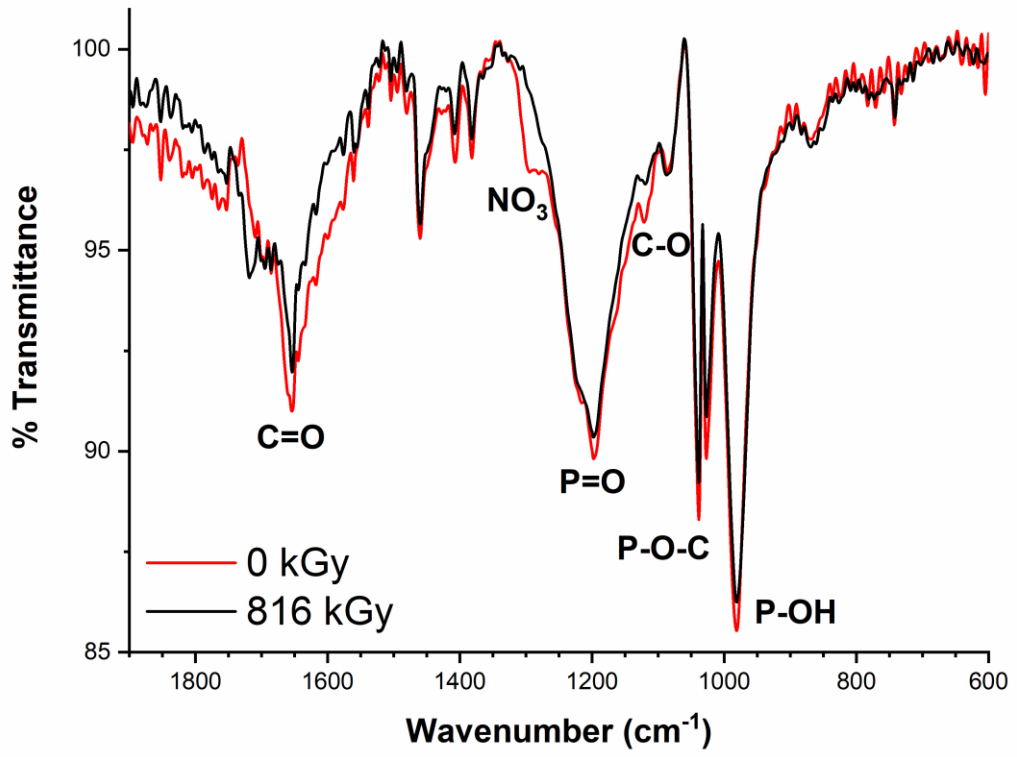

Figure 4. FT-IR spectra of 0.5 M HEH[EHP] + 0.05 M T2EDGA contacted with 3 M HNO_3 before and after low LET gamma irradiation.

The FT-IR spectra of the ALSEP solvent with Nd(III) extracted from 3 M HNO_3 are characterized by shifts to lower energy by the carbonyl C=O stretch from 1664 cm^{-1} to 1608 cm^{-1} and a slight shift of the phosphoryl P=O stretch from 1197 to 1196 cm^{-1}, indicating the interaction of both functional groups, and hence both ligands, with the metal cation (Figure 5, S6a).[71, 74, 87] Although the P–OH stretching frequency decreases slightly in intensity after Nd(III) extraction, and shifts to higher energy, its general presence suggests the HEH[EHP] is not deprotonated in the complex.[76] The presence of the P-OH stretching frequency could also be evidence for the extraction of Nd(III) by a HEH[EHP] dimer, where one HEH[EHP] molecule is deprotonated. Additionally, the stretching frequency attributed to the P–O–C vibration is now present as a single peak, rather than a doublet before Nd(III) extraction, shifting to 983 cm^{-1} after the extraction, suggesting the linkage oxygen is affected by the uptake of Nd(III). Notably, the band at 1295 cm^{-1} corresponding to the presence of nitric acid is also present and is more pronounced and resolved. These spectral details indicate the extraction and complexation of Nd(III) from 3 M HNO_3 involved T2EHDGA, HEH[EHP], and nitrates.[71, 74]

After an absorbed dose of 624 kGy, the carbonyl C=O transmittance peak at 1608 cm^{-1} is no longer present and sharp vibration bands at 1554, 1632, 1654, 1686 and 1718 cm^{-1} are observed (Figure 5, S6b). These vibrational frequencies could correspond to carbonyl group containing degradation products that could be either bound or unbound to Nd(III). The weakening and almost complete disappearance of the band at 1295 cm^{-1} corresponds to the radiolysis of nitric acid, which is likely not part of the Nd(III) complex after irradiation. Most notably, there is an additional shift to lower energy by the phosphoryl P=O vibration, from 1196 to 1194 – 1191 cm^{-1} after irradiation. This shift was not observed in the spectra of the irradiated solution without Nd(III) present (Figure 4), and likely corresponds to additional complexation of HEH[EHP] to Nd(III). Slight shifts are also observed for the P–OH and P–O–C vibrational bands further suggesting changes in coordination to Nd(III) by HEH[EHP]. Due to the greater radiolytic susceptibility of T2EHDGA and the radiolysis of nitric acid, it is possible HEH[EHP] coordinates to Nd(III) during and after irradiation.

Table 3. Vibrational band assignments for the IR spectra of the ALSEP solution, equilibration with 3 M HNO_3, and extraction of Nd(III) from 3 M HNO_3.

	Band Assignments (cm^{-1})					
	C=O	C-O-C	P=O	P-O-C	P-OH	O-N-O
ALSEP	1664	1117	1197	1038	981	
ALSEP + 3 M HNO_3	1652	1120	1197	1038	981	1293
ALSEP + 0.5 M Nd(III)/3 M HNO_3	1608	1119	1196	1036	983	1296

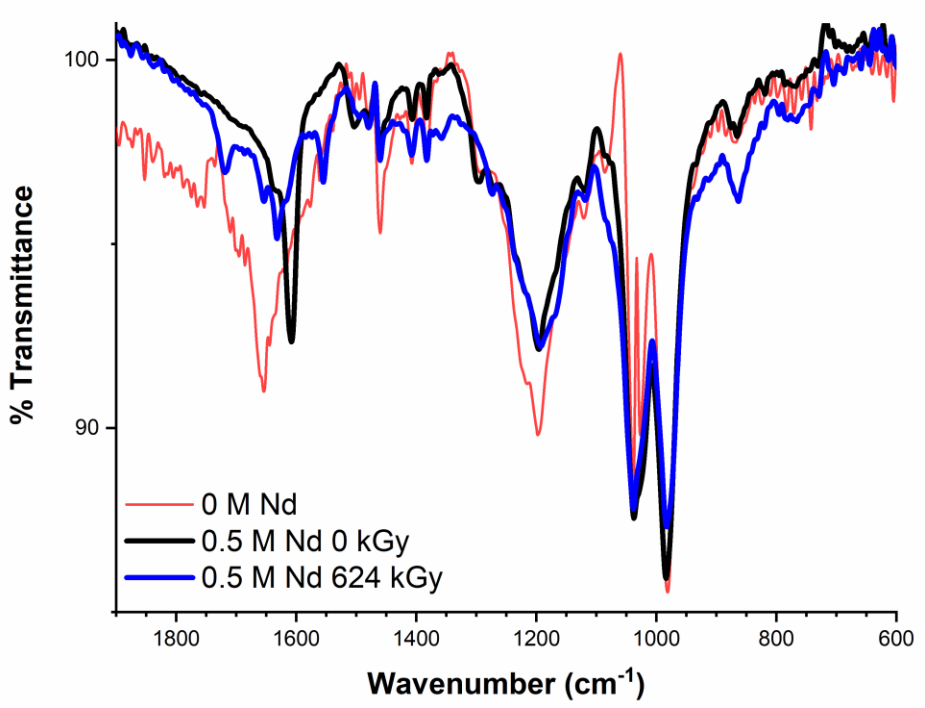

Figure 5. FT-IR spectra of 0.5 M HEH[EHP] + 0.05 M T2EDGA contacted with 0.5 M Nd(III) in 3 M HNO_3 before and after low LET gamma irradiation.

Mass Spectrometry Analysis

Low LET Irradiations of ALSEP solvent

The *m/z* ratios of protonated and sodiated compounds were used to identify parent compounds and degradation products. In all ESI-MS spectra, D will correspond to T2EHDGA and HL and L will correspond to HEH[EHP] and deprotonated HEH[EHP] respectively. The ESI-MS spectra of 0.5

M HEH[EHP] and 0.05 M T2EHDGA is characterized by the protonated peaks of the parent monomer at *m/z* = 307.3 and 581.4, respectively, and protonated dimer of HEH[EHP] at *m/z* = 613.5 (Figure 6a). Impurities likely resulting from the synthesis of T2EHDGA are also present at *m/z* = 130.3 and 242.4, corresponding to 2-ethylhexylamine and bis(2-ethylhexyl)amine. Peaks at *m/z* = 710.2 and 822.3 are assigned to adducts formed between T2EHDGA and the mono and bis(2-ethylhexyl)amine impurities. The negative mode ESI-MS spectra (Figure S8a) is predominantly characterized by the HEH[EHP] monomer parent peak at *m/z* = 305.9, dimer parent peak at *m/z* = 612.2, and organophosphorus impurities (likely from synthesis) at *m/z* = 193.7 (H_2EHP), 321.9 (HDEHP), and 420.1 (DEH[EHP]).[39, 88, 89] The *m/z* at 500.1 in the negative mode ESI-MS spectra (Figure S8a) is assigned to an adduct or condensation product formed between HEH[EHP] and H_2EHP. Table S1 lists the *m/z* peaks detected in positive and negative ESI-MS mode, their assignments, and the conditions of the irradiation.

The ESI-MS spectra of the low LET gamma irradiated solvent shows a significant decrease in the relative abundance of the parent peaks corresponding to T2EHDGA (*m/z* =581) and HEH[EHP] (*m/z* = 306), and a noticeable increase in relative abundance of peaks at *m/z* = 242.5 and 284.4 (Figure 6b). The degradation of tetraalkylamides generally occurs through de-amination (rupture of the N–$C_{carbonyl}$ bond), cleavage of the $C_{methylene}$–O_{ether} and C_{alkyl}–N bonds, and to a lesser extent the $C_{carbonyl}$–$C_{methylene}$ bonds.[31, 34, 35, 55, 56, 90–97] Products from the N–$C_{carbonyl}$ and $C_{methylene}$–O_{ether} bond degradation pathways should include a secondary amine with a molecular weight of 241.5 and an acetamide with a molecular weight of 283.5. We therefore assign the peaks at *m/z* = 242.5 (compound 3 in Scheme 1) and 284.4 (compound 2 in Scheme 1) to correspond to the protonated peaks of the amine and acetamide radiolytic degradation products. Although bis(2-ethylhexyl) amine (*m/z* = 242.5) and mono(2-ethylhexyl)amine (*m/z* = 130.3) are present in the spectra of the non-irradiated ALSEP solvent as likely synthesis impurities, their increase in intensity relative to the decrease in parent peaks confirms the amines as radiolytic products. Although the secondary amine (*m/z* = 242.5) from de-amination is detected, a corresponding aldehyde (compound 5 in Scheme 1) or carboxylic acid (compound 4 in Scheme 1) product from the N–$C_{carbonyl}$ bond rupture is not detected. Although FT-IR data (Figure S4) suggested the presence of multiple carbonyl-group containing compounds after irradiation (1672 – 1720 cm^{-1}), under these conditions neither the aldehyde nor carboxylic acid de-amination products were detected in positive or negative mode, possibly attributed to their low response factor in electrospray ionization mass

spectrometry.[40] The alcohol product (compound 1 in Scheme 1) from the rupturing of the $C_{methylene}$–C_{ether} bond is detected but in very low intensity at *m/z* = 300.5. Furthermore, there was no significant amount of $C_{carbonyl}$–$C_{methylene}$ degradation products detected, consistent with reports citing the rare rupture of that bond.[31, 34, 93, 95] Although previously reported[31], the single de-alkylation product (compound 6 in Scheme 1) is not detected but may be due to low abundance. The ESI-MS spectra of the irradiated solvent also contains peaks at 546.2 (compound 10 in scheme 2) and *m/z* = 434.3 (compound 11 in scheme 2), not present in the spectra of the non-irradiated solvent, and are assigned to condensation products formed between bis(2-ethylhexyl)amine (from de-amination) and HEH[EHP] and mono(2-ethylhexyl)amine and HEH[EHP], respectively, through radical cations recombination.

De-alkylation by scission of the $C_{methylene}$–O_{ether} bond is the primary degradation pathway for alkylphosphoric compounds,[60, 90] as the primary radiolytic degradation product of bis(2-ethylhexyl)phosphoric acid (HDEHP) is the mono(2-ethylhexyl) phosphoric acid (H_2MEHP)[98–100] and similarly for HEH[EHP].[32] The negative mode ESI-MS spectra of irradiated organic solution (Figure S8b) depicts peaks at *m/z* = 193.7 and 207.7, and although *m/z* = 193.7 is present in the non-irradiated solvent as a contaminant, *m/z* = 193.7 is assigned to H_2EHP (compound 9 in scheme 2)[32, 39] and *m/z* = 207.7 is assigned to the radiolytic product from the scission of the C_α–C_β ether carbons (compound 8 in scheme 2).[89]

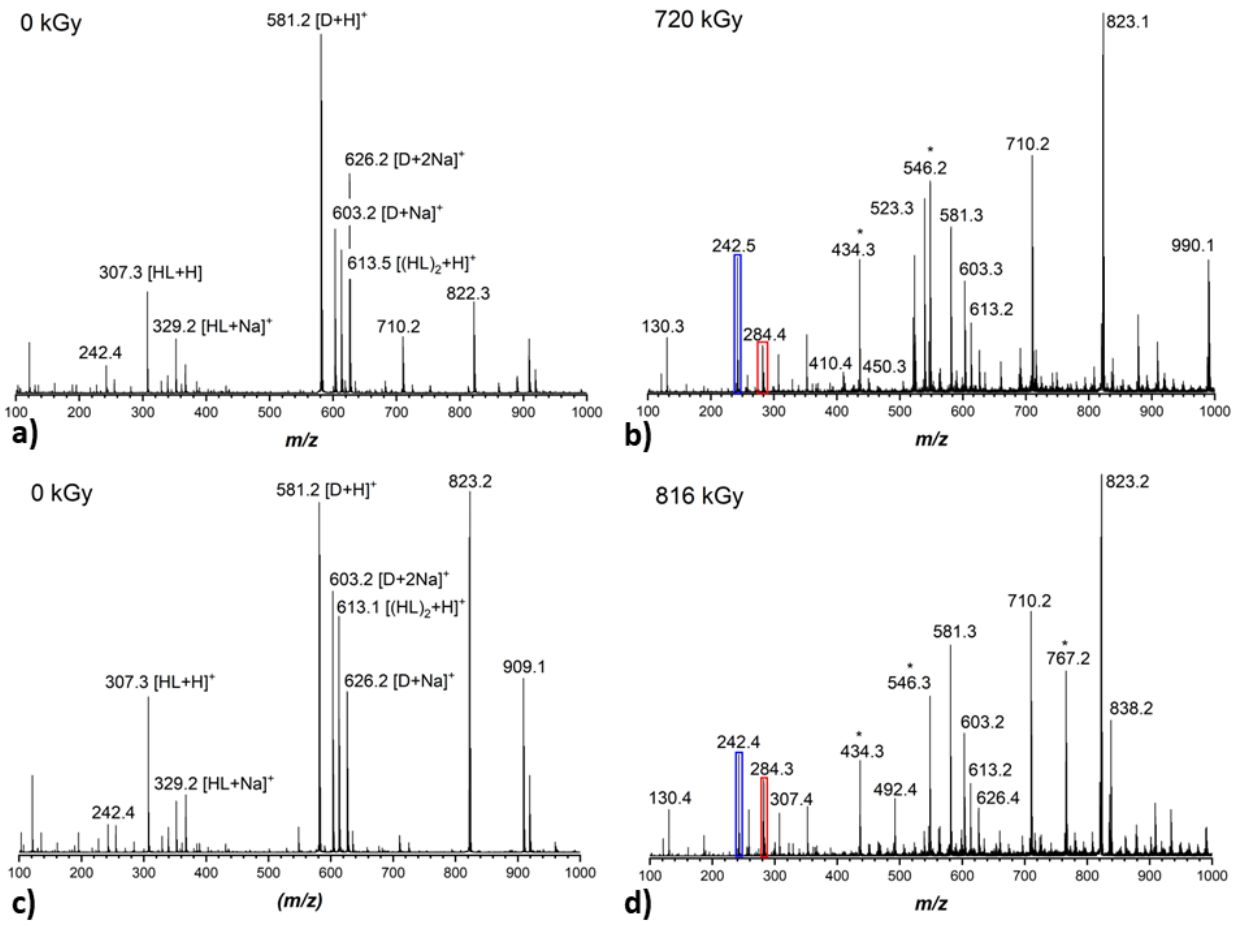

Figure 6. Positive mode ESI-MS spectra of a) ALSEP solvent b) gamma irradiation of ALSEP solvent c) ALSEP pre-equilibrated with nitric acid and d) gamma irradiation of ALSEP pre-equilibrated with nitric acid. Asterisks represent identified radiolytic products.

Low LET Irradiations of ALSEP solvent pre-equilibrated with 3 M HNO_3

Previous studies have reported on preferential bond rupturing of diglycolamides in the presence of high acidity[31, 34, 35, 91, 97], in particular scission of the N–$C_{carbonyl}$.[31, 35] The peak at *m/z* = 767.2 in the ESI-MS spectra of the irradiated nitric acid pre-equilibrated ALSEP solvent (Figure 6d) is not present in the irradiated non pre-equilibrated spectra (Figure 6b). Interestingly, although there was no detection of de-alkylation product (compound 6) nor the alcohol formed after rupturing of the $C_{methylene}$–O_{ether} bond (compound 1) in the irradiated non pre-equilibrated solvent, the peak at *m/z* = 767.2 (compound 7) could correspond to a higher molecular weight compound formed through

the recombination of a de-alkylation and $C_{methylene}$–O_{ether} bond rupture products (Scheme 1). The formation of higher molecular weight compounds formed through the recombination of de-alkylation and alcohol radicals products was also observed in the gamma irradiation of hydrophilic tetraalkylamides.[93, 95] It is likely the alcohol product (2-hydroxyacetamide) (compound 1) is more stable in this acidic system and combines with the de-alkylation product (compound 6) before either undergo further subsequent degradation. Differences in the FT-IR spectra between the irradiated non-acid and acid pre-equilibrated solvent in the 1700 – 1600 cm^{-1} could be due to the higher molecular weight carbonyl containing compounds. This result is in contrast to the radiolysis of a solvent containing CMPO and a monoamide where higher molecular weight products were formed in the absence of an acidic aqueous phase.[52, 53, 84]

High LET Irradiation of ALSEP solvent

In comparison to gamma radiation, high LET radiation sources deposit most of their energy in a short distance allowing for highly localized concentrations of reactive species which can undergo recombination before diffusing into the bulk solution, resulting in higher yields of molecular species and lower radical yields.[60, 101, 102] The effect of alpha radiolysis on the ALSEP solvent was investigated through the $^{10}B(n,\alpha)^{7}Li$ reaction and the following samples were irradiated in the UC Irvine TRIGA Reactor® core:

- ALSEP solvent (Figure 7a, Figure S10a)
- ALSEP solvent containing boron (Figure 7b, Figure S10b)
- ALSEP solvent pre-equilibrated with 3 M HNO_3 (Figure 7c, Figure S11a)
- ALSEP solvent pre-equilibrated with 3 M HNO_3 and containing boron (Figure 7d, Figure S11b)

The radiolysis of irradiated ALSEP solvent samples without dissolved boron is attributed to low LET gamma radiation, and the ESI-MS spectra (Figure 7a, S10a) bears a strong resemblance to that of the ALSEP solvent irradiated in the Cs-137 gamma irradiator cell and therefore identical radiolytic species were identified. Radiolytic products identified in the low LET gamma irradiation of the ALSEP solvent were also present and identified in the ESI-MS spectra of the boron

containing irradiation (Figure 7b) suggesting high alpha LET irradiation does not significantly impact the degradation pathway of the solvent only samples.

High LET Irradiations of ALSEP solvent contacted with 3 M HNO_3

The positive mode ESI-MS spectra (Figure 7c) of the ALSEP solvent pre-equilibrated with 3 M HNO_3 irradiated in the reactor core with no boron present revealed products previously identified in the similar solvent irradiated in the Cs-137 gamma irradiator cell (Figure 6d) including the peak at *m/z* = 767.2 (compound 7), although in low abundance, assigned to the condensation product between the alcohol (compound 1) and de-alkylation product (compound 6). The addition of boron (Figure 7d) also produced similar degradation compounds, and the at peak at *m/z* = 767.2 (compound 7) is present in greater intensity likely due to greater recombination of species in the present of high LET alpha irradiation.

In the negative mode ESI-MS spectra, peaks at *m/z* = 193.6 (compound 9 in scheme 2) and 207.7 (compound 8 in scheme 2) assigned to the cleavage of the $C_{methylene}$–O_{ether} and C_{α}–C_{β} ether bonds were detected in all irradiated samples (Figure S10 – S11). Although they appear in the spectra of all irradiated samples, peaks at *m/z* = 385.9 and 474.4 appear in greater intensity in the samples containing boron (Figure S10b, S11b), and do not appear in the spectra of the non-irradiated samples as possible contaminants (Figure S8), and therefore *m/z* = 385.9 is assigned to the condensation product formed by two H_2EHP ligands (compound 12 in Scheme 2) and *m/z* = 474.4 (compound 13 in Scheme 2) is assigned to a condensation products formed by H_2EHP and the acetamide (compound 13) product from rupturing of the N–$C_{carbonyl}$ bond on the T2EHDGA.

With minor exceptions, the radiolytic degradation products and pathways between low LET gamma and high LET alpha radiolysis of the ALSEP solvent comprised of HEH[EHP] and T2EHDGA are overall similar. Previous reports comparing gamma and alpha radiolytic degradation products of several extractants utilized in solvent extraction processes reached a similar conclusion. High LET irradiation of TBP indicated little difference in the yield of HDBP formed in comparison to gamma irradiation.[60, 103] High LET "*in-situ*" alpha radiolysis of di-ethylhexylbutyramide complexed with Pu(IV) revealed alpha degradation products were similar to those corresponding to gamma irradiation of the free di-ethylhexylbutyramide.[40] Alpha and gamma irradiation of the malonamide DMDOHEMA also produced similar radiolytic degradation products.[64] High LET irradiation studies carried out with TODGA revealed different presumed

degradation products in comparison to low LET gamma irradiation, although degradation products were assigned to alkanes formed through the radiolytic degradation of *n*-dodecane.[37] Although the low LET gamma irradiation of CMPO mostly leads to rupturing of the N–$C_{carbonyl}$ amide bond, alpha irradiation leads to bond rupturing at the P–$C_{methylene}$ and $C_{carbonyl}$–$C_{methylene}$ bonds[52, 62, 104] in addition to N–$C_{carbonyl}$ bond rupturing.[104] In the presented study, the presence of high acidity appeared to favor the formation of higher molecular weight T2EHDGA species after both gamma and alpha irradiation while alpha irradiation appeared to play a role in the formation of high molecular weight HEH[EHP] degradation products.

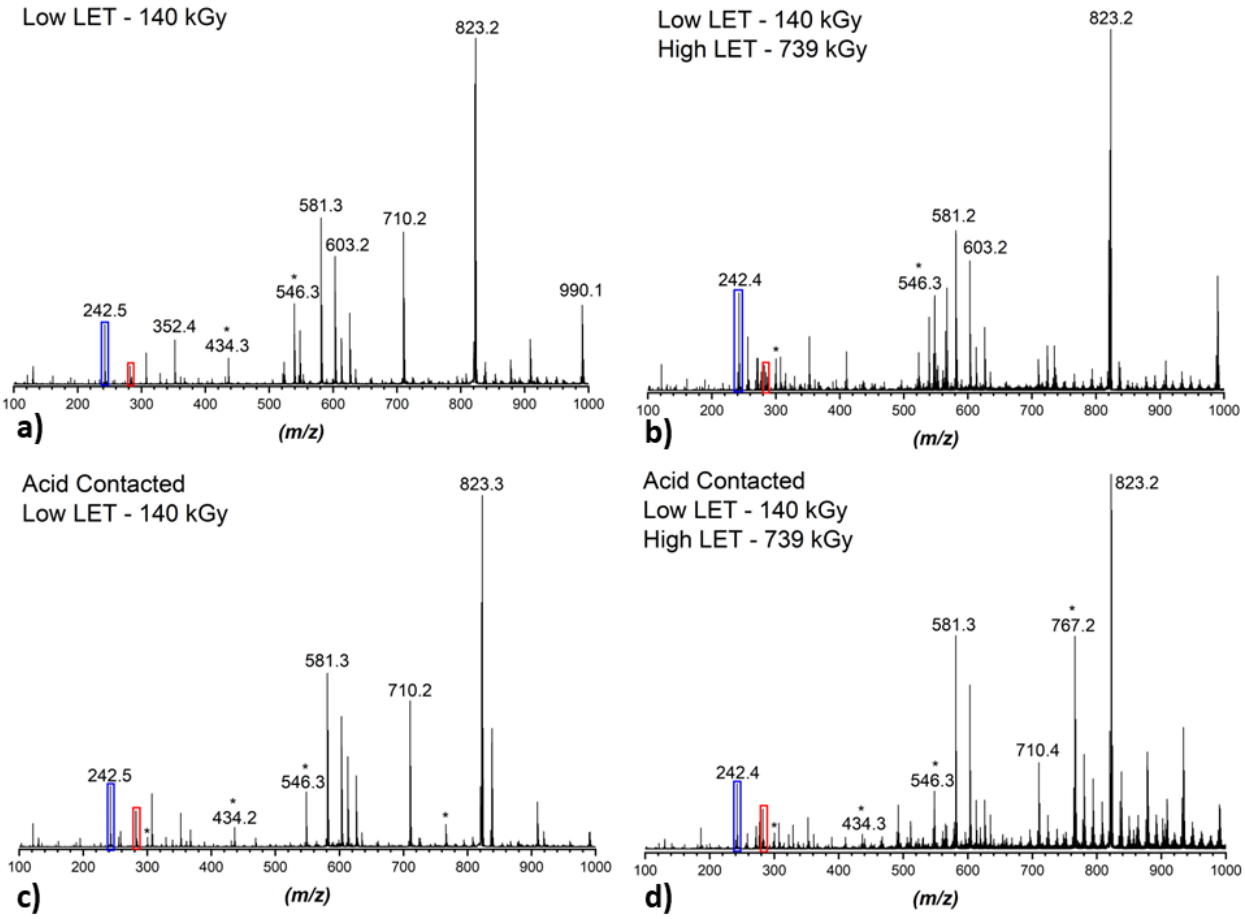

Figure 7. Positive mode ESI-MS of a) ALSEP solvent b) ALSEP solvent containing boron c) ALSEP solvent pre-equilibrated with 3 M HNO_3 and d) ALSEP solvent pre-equilibrated with 3 M HNO_3 containing boron irradiated in the UC Irvine TRIGA Reactor.

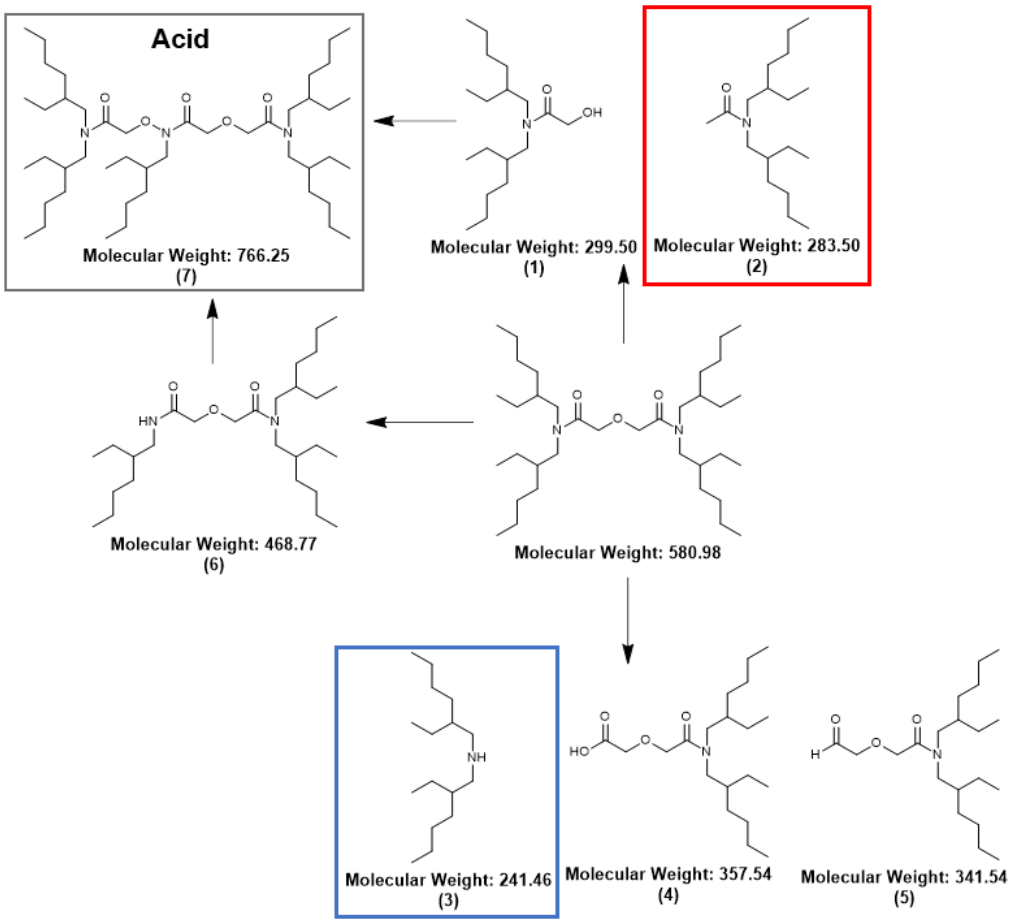

Scheme 1. Proposed overall T2EHDGA radiolytic degradation pathway based on *m/z* detected in positive mode ESI-MS.

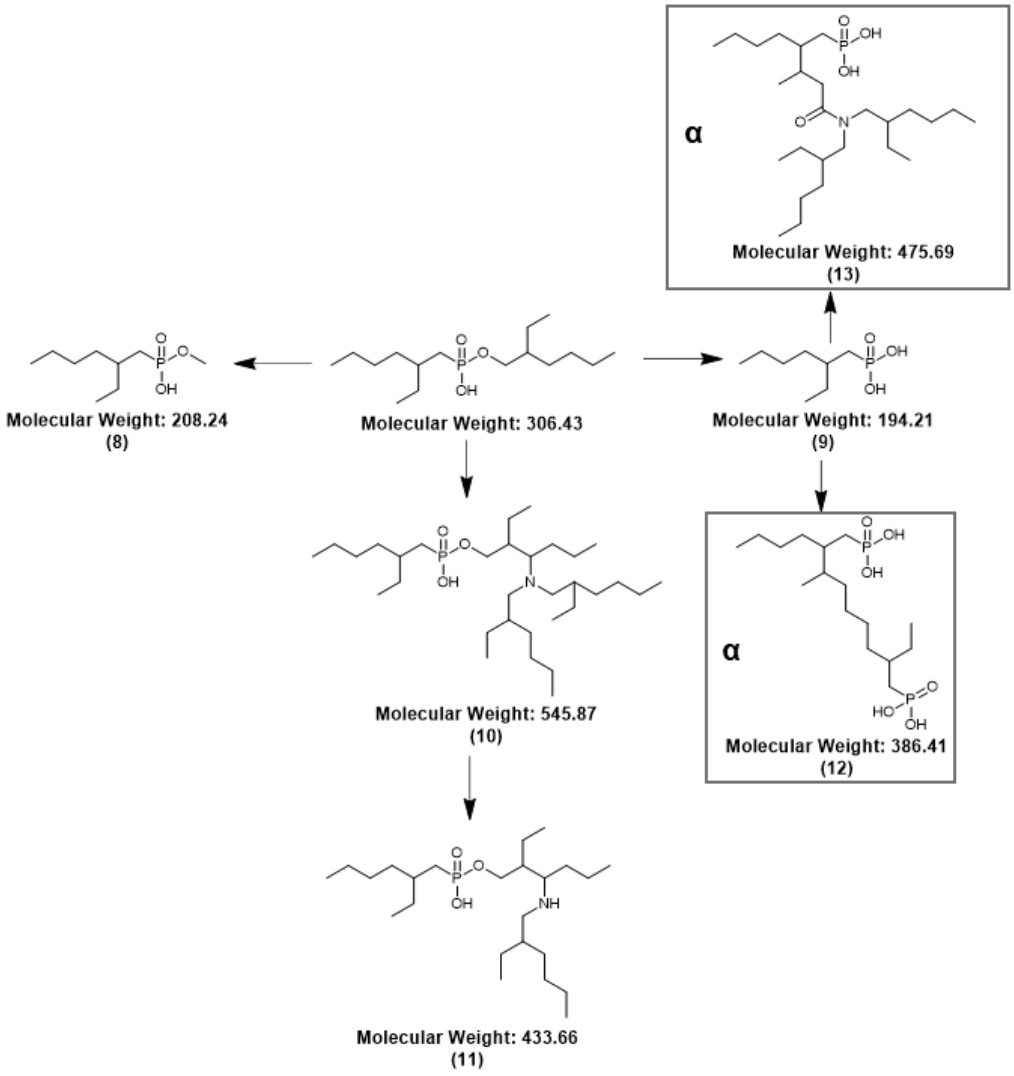

Scheme 2. Proposed overall HEH[EHP] radiolytic degradation pathway bases on *m/z* detected in positive and negative mode ESI-MS.

Low LET Irradiation of Nd-Loaded ALSEP solvent

ESI-MS has proven as a useful technique in elucidating the nature and stoichiometry of ligand-metal complexes in solution, particularly with f-elements complexes.[88, 105–109] ESI-MS has also been applied in determining the stoichiometry of metal complexes formed with mixtures of amides and HDEHP in solvent extraction systems.[71, 75, 110–112] In the cited studies, the ESI-MS spectra of the metal extracted by the ligand mixture were significantly different than spectra corresponding to the metal extracted by the individual ligands, and species in which both ligands were coordinated

to the extracted metal complex were identified. It was concluded the complex $M(NO_3)_x(D)_y(L)_{(3-x)}(HL)_z$ (x = 0 or 1, z = 0, 1, or 2, D = amide, and L = HDEHP) was formed after contact with 0.1 – 0.5 M HNO_3, 1 M HNO_3, and EtOH mixture.[71, 110, 112] Furthermore, recent complexation studies with trivalent f-elements, T2EHDGA, and HEH[EHP] under ALSEP extracting conditions (2 – 4 M HNO_3) concluded the formation of the complex $M(T2EHDGA)_2(HEH[EHP])_2(NO_3)_3$ where fully protonated HEH[EHP] participates in the extracted complex.[73] Although the high acidity inhibits deprotonation of HEH[EHP], the stabilization of the $M(T2EHDGA)_2(HEH[EHP])_2(NO_3)_3$ complex is enhanced by the high HEH[EHP] concentration, strong PO-M bonds, and hydrogen bonding to the nitrate anions.[73]

The positive and negative mode ESI-MS spectra of the ALSEP solvent contacted with 0.5 M Nd in 3 M HNO_3 are shown in Figure 8a and 8b. Additional positive and negative mode spectra of contact with 0.001, 0.01, 0.05, and 0.1 M Nd in 3 M HNO_3 are shown in Figure S12 – S13 in the SI which show increasing relative abundance of higher molecular weight structures with increasing metal concentration. Positive mode ESI-MS spectra revealed the ALSEP solvent contained Nd(III) complexes as $M(T2EHDGA)_2(NO_3)_3$, $M(T2EHDGA)_2(HEH[EHP])_3$, and $M(T2EHDGA)_2(HEH[EHP])_2(NO_3)_3$ (Figure 8a). The presence of 2 T2EHDGA molecules in the extracted metal species is also consistent with stoichiometry obtained through slope-analysis solvent extraction studies.[73, 77] The mixed species could also be forming during the ionization process, as changes in skimmer and cone voltage can alter the stability and abundance of multiple species in mass spectrometry.[71, 75, 113] Additionally, the negative mode ESI-MS spectra (Figure 8b) suggests the presence of the $M(HEH[EHP])(NO_3)$ species, which are likely formed during the ionization process as T2EHDGA and nitrate are replaced by HEH[EHP] molecules. It is also worth noting a peak is detected which would be associated with a $Nd(HEH[EHP])_3$ complex at *m/z* = 1062, a peak at *m/z* = 1362 assigned to $M((HEH[EHP])_3)(HEH[EHP])$, and a peak at *m/z* = 1670 assigned to $M(HEH[EHP])_3(HEH[EHP])_2$, although they are present in low relative abundance and could be formed during the ionization process. A listed of detected *m/z* peaks in positive mode ESI and their assignment of the Nd(III) loaded ALSEP solvent are listed in Table S2 in the SI.

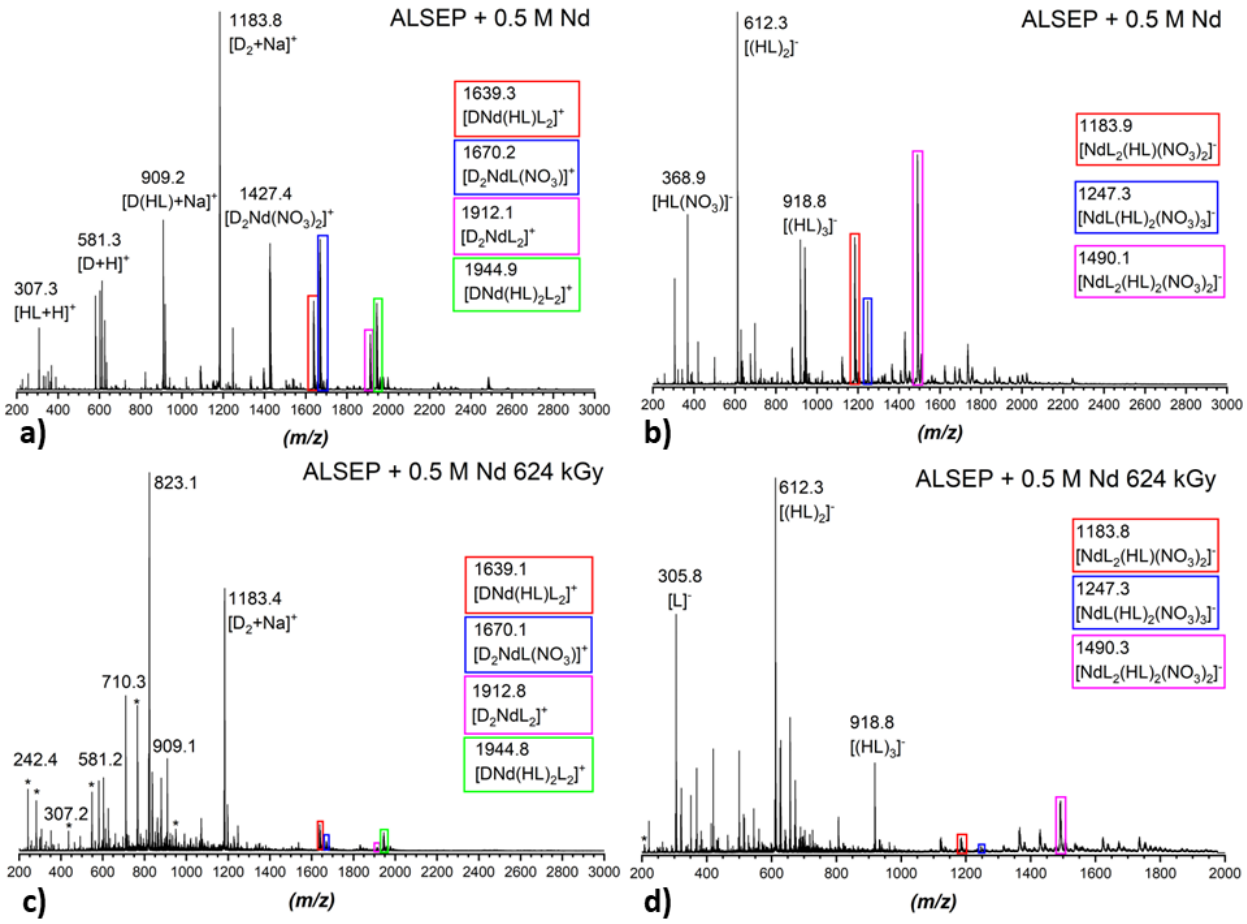

Figure 8. a) Positive b) negative mode of ESI-MS spectra of ALSEP solvent contacted with 0.5 M Nd(III) in 3 M HNO_3. c) Positive and d) negative mode ESI-MS spectra of the irradiation of ALSEP contacted with 0.5 M Nd(III) in 3 M HNO_3.

The positive and negative mode ESI-MS spectra of the low LET gamma irradiation of Nd(III) loaded ALSEP solvent are shown in Figure 8c and 8d, and additional spectra may be found in Figure S14 – S19 in the SI. In the positive mode spectra, the relative intensity of the peaks corresponding to Nd(III) complexes decrease with increasing absorbed dose. Of note, the peak at *m/z* = 1427, assigned to $[M(T2EHDGA)_2(NO_3)_2]^+$, is no longer detected after an absorbed dose of 624 kGy (Figure 8c, S16). The disappearance of this peak, and overall decrease in relative intensity of all Nd(III) complex peaks, is likely attributed to the radiolytic susceptibility of the T2EHDGA ligand. Degradation products detected in the positive mode spectra (Figure 8c) of the irradiated Nd(III) loaded ALSEP solvent were also similar to those detected after the irradiation of 3 M

HNO_3 equilibrated ALSEP solvent (Figure 6d, Table S1). This results is consistent with gamma irradiations of Zr loaded HDEHP and Pu(IV) loaded malonamide where the detected degradation products were similar to those found in the irradiation of the free ligand.[40, 114] In the case of the Zr-HDEHP complex, it was believed the complex decomposed to produce free HDEHP which was subsequently degraded to H_2MEHP.[114] It could be possible T2EHDGA is de-complexed from Nd(III) before underdoing subsequent degradation, as also reported for the irradiation of uranyl-loaded TBP.[41]

The radiolytic degradation of T2EHDGA in the ALSEP solvent occurs through the rupturing of the amide N–$C_{carbonyl}$ bond. Although the formed diamine (compound 3 in scheme 1) is not expected to complex a metal cation and would likely be scrubbed out of the organic phase, the carboxylic acid (compound 4), with coordinating carbonyl groups, will remain organic soluble. Interestingly, there is a small signal at *m/z* = 950 which could correspond to Nd(III) complexed by the carboxylic acid (compound 4) as $[M(D_2)(NO_3)_2]^+$. The peak is not present in the 0 kGy spectra and intensity increases with dose, although it does not become the dominant or most abundant species. The gamma irradiation of a Pu(IV)-malonamide complex also revealed the complexation of Pu(IV) by a degradation product, although the compound was only an unsaturated malonamide.[40] It could be possible the irradiation of the metal loaded ALSEP solvent leads to the dissociation of T2EHDGA from Nd(III), N–$C_{carbonyl}$ bond rupture occurs, followed by complexation of Nd(III) by the carboxylic acid (compound 4).

The intensity of peaks corresponding to complexed Nd(III) also decrease with absorbed dose in the negative mode ESI-MS spectra (Figure 8d, S17 – S19). Given the greater quantity of HEH[EHP] compared to T2EHDGA in the solvent, and the radiolytic robustness of HEH[EHP], the decreasing peak intensity is attributed to T2EHDGA degradation. The intensity decrease follows T2EHDGA degradation as there is less metal bound T2EHDGA for HEH[EHP] to replace during the ionization process. Of note, the intensity of the peak at *m/z* = 223, corresponding to the cleavage of the C_α–C_β ether bonds in HEH[EHP], does not drastically increase with absorbed dose. Although present in low abundance in the spectra of non-irradiated Nd(III) loaded ALSEP solvent, the peaks at *m/z* = 1364, 1427, and 1670, assigned to $[M(HEH[EHP])_3(HEH[EHP])]^-$, $[M(HEH[EHP])_3(HEH[EHP])_2]^-$, and $[M(HEH[EHP])_3(HEH[EHP])(NO_3)]^-$, respectively, are also present in the spectra of the irradiated Nd(III) loaded ALSEP solvent. Taking into consideration

spectral changes observed in the absorption (Figure 3) and vibrational spectroscopy (Figure 5), and the lower abundance of T2EHDGA for HEH[EHP] to replace during the ionization process, these signals (*m/z* = 1364, 1427, and 1670) could correspond to the presence of $Nd(HEH[EHP])_3$ in the solvent after irradiation. Although they are present in small relative intensity in the non-irradiated spectra, their continued presence and abundance relative to other assigned peaks in the irradiated solvent spectra suggests a significant amount of $Nd(HEH[EHP])_3$ could be present in the irradiated organic solvent.

Conclusions

Degradation dose constants revealed greater rate of degradation for T2EHDGA than HEH[EHP] for both low LET gamma and high LET alpha irradiation, although low LET gamma irradiation resulted in greater degradation. Although equilibration with 3 M HNO_3 did not significantly alter the degradation kinetics, it did appear to alter the degradation pathway. Absorption, vibrational, and mass spectra were different between the non-contacted and acid-contacted solutions. Although low LET gamma degradation of the T2EHDGA ligand overall occurred through de-amination and ether linkage rupture, the presence of nitric acid contributed to the formation of high molecular weight, recombination products. Degradation products formed by low and high LET radiation were similar, although recombination products between HEH[EHP] degradation products were formed in the presence of high LET irradiation. The extraction of Nd(III) by the ALSEP solvent is believed to take place through the formation of a $Nd(T2EHDGA)(HEH[EHP])(NO_3)$ complex. Absorption and vibrational spectroscopy suggested both ligands were involved in the coordination of Nd(III). Although the same degradation products are formed in the Nd(III) saturated ALSEP solvent as with Nd(III) not present in the solvent, a Nd-HEH[EHP] only complex appears to form with increasing absorbed dose as T2EHDGA undergoes significant decomposition. The formation of this complex may result in difficulties scrubbing or stripping the metal ions from irradiated solutions in the ALSEP process. This result could also occur with solvents consisting of multiple extractants, in particular those consisting of organophosphorus extractants. Degradation rates for the metal loaded ALSEP solvent could also be investigated in order to thoroughly understand the degradation mechanism that occurs in the ALSEP system.

Acknowledgements

This work was performed under the auspices of the U.S. Department of Energy by Lawrence Livermore National Laboratory under contract DE-AC52-07NA27344.

References

[1] Woodhead Publishing Series in Energy. In *Advanced Separation Techniques for Nuclear Fuel Reprocessing and Radioactive Waste Treatment*; Nash, K. L., Lumetta, G. J., Eds.; Woodhead Publishing, 2011; pp xiv–xvii. https://doi.org/10.1016/B978-1-84569-501-9.50019-0.

[2] Todd, T. A.; Wigeland, R. A. Advanced Separation Technologies for Processing Spent Nuclear Fuel and the Potential Benefits to a Geologic Repository. In *Separations for the Nuclear Fuel Cycle in the 21st Century*; ACS Symposium Series; American Chemical Society, 2006; Vol. 933, pp 41–55. https://doi.org/10.1021/bk-2006-0933.ch003.

[3] Lanham, W. B.; Runion, T. C. *PUREX Process for Plutonium and Uranium Recovery*; United States, 1949. https://doi.org/10.2172/4165457.

[4] Grenthe, I.; Drożdżyński, J.; Fujino, T.; Buck, E. C.; Albrecht-Schmitt, T. E.; Wolf, S. F. Uranium. In *The Chemistry of the Actinide and Transactinide Elements*; Morss, L. R., Edelstein, N. M., Fuger, J., Eds.; Springer Netherlands: Dordrecht, 2006; pp 253–698. https://doi.org/10.1007/1-4020-3598-5_5.

[5] Clark, D. L.; Hecker, S. S.; Jarvinen, G. D.; Neu, M. P. Plutonium. In *The Chemistry of the Actinide and Transactinide Elements*; Morss, L. R., Edelstein, N. M., Fuger, J., Eds.; Springer Netherlands: Dordrecht, 2006; pp 813–1264. https://doi.org/10.1007/1-4020-3598-5_7.

[6] Nash, K. L. A Review of the Basic Chemistry and Recent Developments in Trivalent F-Elements Separations. *Solvent Extr. Ion Exch.*, **1993**, *11* (4), 729–768. https://doi.org/10.1080/07366299308918184.

[7] Salvatores, M.; Palmiotti, G. Radioactive Waste Partitioning and Transmutation within Advanced Fuel Cycles: Achievements and Challenges. *Prog. Part. Nucl. Phys.*, **2011**, *66* (1), 144–166. https://doi.org/10.1016/j.ppnp.2010.10.001.

[8] Weaver, B.; Kappelmann, F. A. *TALSPEAK: A New Method of Separating Americium and Curium From The Lanthanides by Extraction from an Aqueous Solution of an Aminopolyacetic Acid Complex With a Monoacidic Organophosphate or Phosphonate*; United States, 1964. https://doi.org/10.2172/4028257.

[9] Philip Horwitz, E.; Kalina, D. C.; Diamond, H.; Vandegrift, G. F.; Schulz, W. W. The TRUEX Process - A Process for the Extraction of the Transuranic Elements from Nitric Acid in Wastes Utilizing Modified PUREX Solvent. *Solvent Extr. Ion Exch.*, **1985**, *3* (1–2), 75–109. https://doi.org/10.1080/07366298508918504.

[10] Daniel Serrano-Purroy; P. Baron; Birgit Christiansen; R. Malmbeck; C. Sorel; J.-P. Glatz. Recovery of Minor Actinides from HLLW Using the DIAMEX Process. *Radiochim. Acta*, **2005**, *93* (6), 351–355. https://doi.org/10.1524/ract.93.6.351.65642.

[11] Hill, C.; Guillaneux, D.; Berthon, L.; Madic, C. Sanex-Btp Process Development Studies. *J. Nucl. Sci. Technol.*, **2002**, *39* (sup3), 309–312. https://doi.org/10.1080/00223131.2002.10875470.

[12] Mathur, J. N.; Murali, M. S.; Nash, K. L. Actinide Partitioning - A Review. *Solvent Extr. Ion Exch.*, **2001**, *19* (3), 357–390. https://doi.org/10.1081/SEI-100103276.

[13] Carrott, M.; Bell, K.; Brown, J.; Geist, A.; Gregson, C.; Hères, X.; Maher, C.; Malmbeck, R.; Mason, C.; Modolo, G.; et al. Development of a New Flowsheet for Co-Separating the Transuranic Actinides: The "EURO-GANEX" Process. *Solvent Extr. Ion Exch.*, **2014**, *32* (5), 447–467. https://doi.org/10.1080/07366299.2014.896580.

[14] Carrott, M.; Geist, A.; Hères, X.; Lange, S.; Malmbeck, R.; Miguirditchian, M.; Modolo, G.; Wilden, A.; Taylor, R. Distribution of Plutonium, Americium and Interfering Fission Products between Nitric Acid and a Mixed Organic Phase of TODGA and DMDOHEMA in Kerosene, and Implications for the Design of the "EURO-GANEX" Process. *Hydrometallurgy*, **2015**, *152*, 139–148. https://doi.org/10.1016/j.hydromet.2014.12.019.

[15] Malmbeck, R.; Magnusson, D.; Geist, A. Modified Diglycolamides for Grouped Actinide Separation. *J. Radioanal. Nucl. Chem.*, **2017**, *314* (3), 2531–2538. https://doi.org/10.1007/s10967-017-5614-2.

[16] Lumetta, G. J.; Gelis, A. V.; Carter, J. C.; Niver, C. M.; Smoot, M. R. The Actinide-Lanthanide Separation Concept. *Solvent Extr. Ion Exch.*, **2014**, *32* (4), 333–347. https://doi.org/10.1080/07366299.2014.895638.

[17] Gelis, A. V.; Lumetta, G. J. Actinide Lanthanide Separation Process—ALSEP. *Ind. Eng. Chem. Res.*, **2014**, *53* (4), 1624–1631. https://doi.org/10.1021/ie403569e.

[18] Ansari, S. A.; Pathak, P. N.; Manchanda, V. K.; Husain, M.; Prasad, A. K.; Parmar, V. S. N,N,N',N'-Tetraoctyl Diglycolamide (TODGA): A Promising Extractant for Actinide-Partitioning from High-Level Waste (HLW). *Solvent Extr. Ion Exch.*, **2005**, *23* (4), 463–479. https://doi.org/10.1081/SEI-200066296.

[19] Sasaki, Y.; Sugo, Y.; Suzuki, S.; Tachimori, S. The Novel Extractants, Diglycolamides, for the Extraction of Lanthanides and Actinides in HNO3-n-Dodecane System. *Solvent Extr. Ion Exch.*, **2001**, *19* (1), 91–103. https://doi.org/10.1081/SEI-100001376.

[20] Whittaker, D.; Geist, A.; Modolo, G.; Taylor, R.; Sarsfield, M.; Wilden, A. Applications of Diglycolamide Based Solvent Extraction Processes in Spent Nuclear Fuel Reprocessing, Part 1: TODGA. *Solvent Extr. Ion Exch.*, **2018**, *36* (3), 223–256. https://doi.org/10.1080/07366299.2018.1464269.

[21] Gasparini, G. M.; Grossi, G. Review Articles Long Chain Disubstituted Aliphatic Amides as Extracting Agents in Industrial Applications of Solvent Extraction. *Solvent Extr. Ion Exch.*, **1986**, *4* (6), 1233–1271. https://doi.org/10.1080/07366298608917921.

[22] Siddall, T. H. I. *Bidentate Organophosphorus Compounds as Extractants. I. Extraction of Cerium, Promethium, and Americium Nitrates*; United States, 1962.

[23] Nilsson, M.; Nash, K. L. Review Article: A Review of the Development and Operational Characteristics of the TALSPEAK Process. *Solvent Extr. Ion Exch.*, **2007**, *25* (6), 665–701. https://doi.org/10.1080/07366290701634636.

[24] Kosyakov, V. N.; Yerin, E. A. Separation of Transplutonium and Rare-Earth Elements by Extraction with HDEHP from DTPA Solutions. *J. Radioanal. Chem.*, **1978**, *43* (1), 37–51. https://doi.org/10.1007/BF02519439.

[25] Runde, W. H.; Schulz, W. W. Americium. In *The Chemistry of the Actinide and Transactinide Elements*; Morss, L. R., Edelstein, N. M., Fuger, J., Eds.; Springer Netherlands: Dordrecht, 2006; pp 1265–1395. https://doi.org/10.1007/1-4020-3598-5_8.

[26] Lumetta, G. J.; Thompson, M. C.; Penneman, R. A.; Eller, P. G. Curium. In *The Chemistry of the Actinide and Transactinide Elements*; Morss, L. R., Edelstein, N. M., Fuger, J., Eds.; Springer Netherlands: Dordrecht, 2006; pp 1397–1443. https://doi.org/10.1007/1-4020-3598-5_9.

[27] J. N. Sharma; R. Ruhela; K. K. Singh; Manoj Kumar; C. Janardhanan; P. V. Achutan; S. Manohar; P. K. Wattal; A. K. Suri. Studies on Hydrolysis and Radiolysis of Tetra(2-Ethylhexyl)Diglycolamide (TEHDGA)/Isodecyl Alcohol/n-Dodecane Solvent System. *Radiochim. Acta*, **2010**, *98* (8), 485–491. https://doi.org/10.1524/ract.2010.1749.

[28] Gujar, R. B.; Ansari, S. A.; Murali, M. S.; Mohapatra, P. K.; Manchanda, V. K. Comparative Evaluation of Two Substituted Diglycolamide Extractants for 'Actinide Partitioning.' *J. Radioanal. Nucl. Chem.*, **2010**, *284* (2), 377–385. https://doi.org/10.1007/s10967-010-0467-y.

[29] Deepika, P.; Sabharwal, K. N.; Srinivasan, T. G.; Vasudeva Rao, P. R. Studies on the Use of N,N,N′,N′-Tetra(2-Ethylhexyl) Diglycolamide (TEHDGA) for Actinide Partitioning. I: Investigation on Third-Phase Formation and Extraction Behavior. *Solvent Extr. Ion Exch.*, **2010**, *28* (2), 184–201. https://doi.org/10.1080/07366290903565885.

[30] Deepika, P.; Sabharwal, K. N.; Srinivasan, T. G.; Vasudeva Rao, P. R. Studies on the Use of N,N,N′,N′-Tetra(2-Ethylhexyl) Diglycolamide (TEHDGA) for Actinide Partitioning II: Investigation on Radiolytic Stability. *Solvent Extr. Ion Exch.*, **2011**, *29* (2), 230–246. https://doi.org/10.1080/07366299.2011.539145.

[31] Zarzana, C. A.; Groenewold, G. S.; Mincher, B. J.; Mezyk, S. P.; Wilden, A.; Schmidt, H.; Modolo, G.; Wishart, J. F.; Cook, A. R. A Comparison of the γ-Radiolysis of TODGA and T(EH)DGA Using UHPLC-ESI-MS Analysis. *Solvent Extr. Ion Exch.*, **2015**, *33* (5), 431–447. https://doi.org/10.1080/07366299.2015.1012885.

[32] Peterman, D. R. [Idaho N. Lab. (INL), Idaho Falls, ID (United States)]; McDowell, R. G. [Idaho N. Lab. (INL), Idaho Falls, ID (United States)]; Zarzana, C. A. [Idaho N. Lab. (INL), Idaho Falls, ID (United States)]; Johnson, K. M. [Idaho N. Lab. (INL), Idaho Falls, ID (United States)]; Rowe, S. M. [Idaho N. Lab. (INL), Idaho Falls, ID (United States)]; Groenewold, G. S. [Idaho N. Lab. (INL), Idaho Falls, ID (United States)]. *Investigation of the Hydrolytic and Radiolytic Degradation of HEH[EHP]*; United States, 2016. https://doi.org/10.2172/1406972.

[33] Peterman, D. R.; Zarzana, C. A.; Tillotson, R. D.; McDowell, R. G.; Rae, C.; Groenewold, G. S.; Law, J. D. Evaluation of the Impacts of Gamma Radiolysis on an ALSEP Process Solvent. *J. Radioanal. Nucl. Chem.*, **2018**, *316* (2), 855–860. https://doi.org/10.1007/s10967-018-5737-0.

[34] Sugo Y.; Sasaki Y.; Tachimori S. Studies on Hydrolysis and Radiolysis of N,N,N′,N′-Tetraoctyl-3-Oxapentane-1,5-Diamide. *Radiochim. Acta*, **2009**, *90* (3), 161. https://doi.org/10.1524/ract.2002.90.3_2002.161.

[35] Verlinden, B.; Van Hecke, K.; Wilden, A.; Hupert, M.; Santiago-Schübel, B.; Egberink, R. J. M.; Verboom, W.; Kowalski, P. M.; Modolo, G.; Verwerft, M.; et al. Gamma Radiolytic Stability of the Novel Modified Diglycolamide 2,2′-Oxybis(N,N-Didecylpropanamide) (MTDDGA) for Grouped Actinide Extraction. *RSC Adv.*, **2022**, *12* (20), 12416–12426. https://doi.org/10.1039/D1RA08761D.

[36] Mezyk, S. P.; Horne, G. P.; Mincher, B. J.; Zalupski, P. R.; Cook, A. R.; Wishart, J. F. The Chemistry of Separations Ligand Degradation by Organic Radical Cations. *ATALANTE 2016 Int. Conf. Nucl. Chem. Sustain. Fuel Cycles*, **2016**, *21*, 61–65. https://doi.org/10.1016/j.proche.2016.10.009.

[37] Sugo, Y.; Taguchi, M.; Sasaki, Y.; Hirota, K.; Kimura, T. Radiolysis Study of Actinide Complexing Agent by Irradiation with Helium Ion Beam. *APSRC-2008 Second Asia-Pac. Symp. Radiat. Chem. August 29 – Sept. 1 2008*, **2009**, *78* (12), 1140–1144. https://doi.org/10.1016/j.radphyschem.2009.06.031.

[38] Malmbeck, R.; Banik, N. L. Radiolytic Behaviour of a TODGA Based Solvent under Alpha Irradiation. *J. Radioanal. Nucl. Chem.*, **2020**, *326* (3), 1609–1615. https://doi.org/10.1007/s10967-020-07444-7.

[39] Holfeltz, V. E.; Campbell, E. L.; Peterman, D. R.; Standaert, R. F.; Paulenova, A.; Lumetta, G. J.; Levitskaia, T. G. Effect of HEH[EHP] Impurities on the ALSEP Solvent Extraction Process. *Solvent Extr. Ion Exch.*, **2018**, *36* (1), 22–40. https://doi.org/10.1080/07366299.2017.1412111.

[40] Drader, J. A.; Boubals, N.; Camès, B.; Guillaumont, D.; Guilbaud, P.; Saint-Louis, G.; Berthon, L. Radiolytic Stability of N,N-Dialkyl Amide: Effect on Pu(Iv) Complexes in Solution. *Dalton Trans.*, **2018**, *47* (1), 251–263. https://doi.org/10.1039/C7DT03447D.

[41] Ngelale, R.; Lee, C.; Bustillos, S.; Nilsson, M. Radiolytic Degradation of Uranyl-Loaded Tributyl Phosphate by High and Low LET Radiation. *Solvent Extr. Ion Exch.*, **2019**, *37* (1), 38–52. https://doi.org/10.1080/07366299.2018.1552549.

[42] Shannon, R. D. Revised Effective Ionic Radii and Systematic Studies on Interatomic Distances in Halides and Chalcogenides. *Acta Crystallogr. Sect. A*, **1976**, *A32*, 751–767.
[43] Traeger, J. C. Electrospray Mass Spectrometry of Organometallic Compounds. *Vol. 200 State Field We Move New Millenium*, **2000**, *200* (1), 387–401. https://doi.org/10.1016/S1387-3806(00)00346-8.
[44] Di Marco, V. B.; Bombi, G. G. Electrospray Mass Spectrometry (ESI-MS) in the Study of Metal–Ligand Solution Equilibria. *Mass Spectrom. Rev.*, **2006**, *25* (3), 347–379. https://doi.org/10.1002/mas.20070.
[45] Pearson, J.; Jan, O.; Miller, G. E.; Nilsson, M. Studies of High Linear Energy Transfer Dosimetry by 10B(n,α)7Li Reactions in Aqueous and Organic Solvents. *J. Radioanal. Nucl. Chem.*, **2012**, *292* (2), 719–727. https://doi.org/10.1007/s10967-011-1479-y.
[46] Pearson, J.; Jan, O.; Wariner, A.; Miller, G. E.; Nilsson, M. Development of a Method for High LET Irradiation of Liquid Systems. *J. Radioanal. Nucl. Chem.*, **2013**, *298* (2), 1401–1409. https://doi.org/10.1007/s10967-013-2549-0.
[47] Pearson, J.; Nilsson, M. Radiolysis of Tributyl Phosphate by Particles of High Linear Energy Transfer. *Solvent Extr. Ion Exch.*, **2014**, *32* (6), 584–600. https://doi.org/10.1080/07366299.2014.924305.
[48] Jayson, G. G.; Parsons, B. J.; Swallow, A. J. The Mechanism of the Fricke Dosimeter. *Int. J. Radiat. Phys. Chem.*, **1975**, *7* (2), 363–370. https://doi.org/10.1016/0020-7055(75)90075-3.
[49] Pearson, J.; Jan, O.; Miller, G.; Nilsson, M. A Comparison of Low and High LET (Linear Energy Transfer) Induced Radiolysis of Solvent Extraction Processes. *ATALANTE 2012 Int. Conf. Nucl. Chem. Sustain. Fuel Cycles*, **2012**, *7*, 334–340. https://doi.org/10.1016/j.proche.2012.10.053.
[50] Mincher, B. J.; Zarzana, C. A.; Mezyk, S. P. *Radical Cations and Acid Protection during Radiolysis*; United States, 2016. https://doi.org/10.2172/1389193.
[51] Mincher, B. J.; Curry, R. D. Considerations for Choice of a Kinetic Fig. of Merit in Process Radiation Chemistry for Waste Treatment. *Appl. Radiat. Isot.*, **2000**, *52* (2), 189–193. https://doi.org/10.1016/S0969-8043(99)00161-X.
[52] Mincher, B. J.; Mezyk, S. P.; Groenewold, G. S. The Radiolysis of CMPO: Effects of Acid, Metal Complexation and Alpha vs. Gamma Radiation. *ATALANTE 2016 Int. Conf. Nucl. Chem. Sustain. Fuel Cycles*, **2016**, *21*, 66–73. https://doi.org/10.1016/j.proche.2016.10.010.
[53] Mincher, B. J.; Mezyk, S. P.; Elias, G.; Groenewold, G. S.; Riddle, C. L.; Olson, L. G. The Radiation Chemistry of CMPO: Part 1. Gamma Radiolysis. *Solvent Extr. Ion Exch.*, **2013**, *31* (7), 715–730. https://doi.org/10.1080/07366299.2013.815491.
[54] Mezyk, S. P.; Mincher, B. J.; Ekberg, C.; Skarnemark, G. Alpha and Gamma Radiolysis of Nuclear Solvent Extraction Ligands Used for An(III) and Ln(III) Separations. *J. Radioanal. Nucl. Chem.*, **2013**, *296* (2), 711–715. https://doi.org/10.1007/s10967-012-2036-z.
[55] Galán, H.; Zarzana, C. A.; Wilden, A.; Núñez, A.; Schmidt, H.; Egberink, R. J. M.; Leoncini, A.; Cobos, J.; Verboom, W.; Modolo, G.; et al. Gamma-Radiolytic Stability of New Methylated TODGA Derivatives for Minor Actinide Recycling. *Dalton Trans.*, **2015**, *44* (41), 18049–18056. https://doi.org/10.1039/C5DT02484F.
[56] Roscioli-Johnson, K. M.; Zarzana, C. A.; Groenewold, G. S.; Mincher, B. J.; Wilden, A.; Schmidt, H.; Modolo, G.; Santiago-Schübel, B. A Study of the γ-Radiolysis of N,N-Didodecyl-N′,N′-Dioctyldiglycolamide Using UHPLC-ESI-MS Analysis. *Solvent Extr. Ion Exch.*, **2016**, *34* (5), 439–453. https://doi.org/10.1080/07366299.2016.1212540.
[57] Spinks, J. W. T.; Woods, R. J. *An Introduction to Radiation Chemistry*; New York, NY (USA); John Wiley and Sons Inc.: United States, 1990.

[58] Mezyk, S. P.; Mincher, B. J.; Dhiman, S. B.; Layne, B.; Wishart, J. F. The Role of Organic Solvent Radical Cations in Separations Ligand Degradation. *J. Radioanal. Nucl. Chem.*, **2016**, *307* (3), 2445–2449. https://doi.org/10.1007/s10967-015-4582-7.

[59] Mincher Bruce J.; Mezyk Stephen P. Radiation Chemical Effects on Radiochemistry: A Review of Examples Important to Nuclear Power. *Radiochim. Acta Int. J. Chem. Asp. Nucl. Sci. Technol.*, **2009**, *97* (9), 519. https://doi.org/10.1524/ract.2009.1646.

[60] Mincher, B. J.; Modolo, G.; Mezyk, S. P. Review Article: The Effects of Radiation Chemistry on Solvent Extraction: 1. Conditions in Acidic Solution and a Review of TBP Radiolysis. *Solvent Extr. Ion Exch.*, **2009**, *27* (1), 1–25. https://doi.org/10.1080/07366290802544767.

[61] Horne, G. P.; Zarzana, C. A.; Grimes, T. S.; Rae, C.; Ceder, J.; Mezyk, S. P.; Mincher, B. J.; Charbonnel, M.-C.; Guilbaud, P.; Saint-Louis, G.; et al. Effect of Chemical Environment on the Radiation Chemistry of N,N-Di-(2-Ethylhexyl)Butyramide (DEHBA) and Plutonium Retention. *Dalton Trans.*, **2019**, *48* (38), 14450–14460. https://doi.org/10.1039/C9DT02383F.

[62] Mincher, B. J.; Mezyk, S. P.; Elias, G.; Groenewold, G. S.; LaVerne, J. A.; Nilsson, M.; Pearson, J.; Schmitt, N. C.; Tillotson, R. D.; Olson, L. G. The Radiation Chemistry of CMPO: Part 2. Alpha Radiolysis. *Solvent Extr. Ion Exch.*, **2014**, *32* (2), 167–178. https://doi.org/10.1080/07366299.2013.850300.

[63] D. Magnusson; Birgit Christiansen; Rikard Malmbeck; Jean-Paul Glatz. Investigation of the Radiolytic Stability of a CyMe4-BTBP Based SANEX Solvent. *Radiochim. Acta*, **2009**, *97* (9), 497–502. https://doi.org/10.1524/ract.2009.1647.

[64] Camès, B.; Bisel, I.; Baron, P.; Hill, C.; Rudloff, D.; Saucerotte, B. DIAMEX Solvent Behavior under Continuous Degradation and Regeneration Operations. In *Nuclear Energy and the Environment*; ACS Symposium Series; American Chemical Society, 2010; Vol. 1046, pp 255–269. https://doi.org/10.1021/bk-2010-1046.ch021.

[65] Bibler, N. E. Gamma and Alpha Radiolysis of Aqueous Solutions of Diethylenetriaminepentaacetic Acid. *J. Inorg. Nucl. Chem.*, **1972**, *34* (4), 1417–1425. https://doi.org/10.1016/0022-1902(72)80342-7.

[66] Pastina, B.; LaVerne, J. A. Hydrogen Peroxide Production in the Radiolysis of Water with Heavy Ions. *J. Phys. Chem. A*, **1999**, *103* (11), 1592–1597. https://doi.org/10.1021/jp984433o.

[67] Choppin, G. R.; Henrie, D. E.; Buijs, K. Environmental Effects on F-f Transitions. I. Neodymium(III). *Inorg. Chem.*, **1966**, *5* (10), 1743–1748. https://doi.org/10.1021/ic50044a023.

[68] Seminara, A.; Musumeci, A. Absorption and Emission Spectra of Neodymium(III) and Europium(III) Complexes. *Inorganica Chim. Acta*, **1984**, *95* (6), 291–307. https://doi.org/10.1016/S0020-1693(00)84898-7.

[69] Stephens, E. M.; Schoene, K.; Richardson, F. S. Hypersensitivity in the 4f .Fwdarw. 4f Absorption Spectra of Neodymium(III) Complexes in Aqueous Solution. *Inorg. Chem.*, **1984**, *23* (12), 1641–1648. https://doi.org/10.1021/ic00180a004.

[70] Jensen, M. P.; Chiarizia, R.; Urban, V. Investigation of the Aggregation of the Neodymium Complexes of Dialkyl Diphosphoric, -Oxothiophosphinic, and -Dithiophosphinic Acids in Toluene. *Solvent Extr. Ion Exch.*, **2001**, *19* (5), 865–884. https://doi.org/10.1081/SEI-100107027.

[71] Muller, J. M.; Berthon, C.; Couston, L.; Zorz, N.; Simonin, J.-P.; Berthon, L. Extraction of Lanthanides(III) by a Mixture of a Malonamide and a Dialkyl Phosphoric Acid. *Solvent Extr. Ion Exch.*, **2016**, *34* (2), 141–160. https://doi.org/10.1080/07366299.2015.1135030.

[72] Ansari, A. A.; Ilmi, R.; Iftikhar, K. Hypersensitivity in the 4f–4f Absorption Spectra of Tris (Acetylacetonato) Neodymium(III) Complexes with Imidazole and Pyrazole in Non-Aqueous Solutions. Effect of Environment on Hypersensitive Transitions. *J. Lumin.*, **2012**, *132* (1), 51–60. https://doi.org/10.1016/j.jlumin.2011.06.054.

[73] Picayo, G. A.; Etz, B. D.; Vyas, S.; Jensen, M. P. Characterization of the ALSEP Process at Equilibrium: Speciation and Stoichiometry of the Extracted Complex. *ACS Omega*, **2020**. https://doi.org/10.1021/acsomega.0c00209.

[74] Hall, G. B.; Holfeltz, V. E.; Campbell, E. L.; Boglaienko, D.; Lumetta, G. J.; Levitskaia, T. G. Evolution of Acid-Dependent Am3+ and Eu3+ Organic Coordination Environment: Effects on the Extraction Efficiency. *Inorg. Chem.*, **2020**, *59* (7), 4453–4467. https://doi.org/10.1021/acs.inorgchem.9b03612.

[75] Muller, J. M.; Berthon, C.; Couston, L.; Guillaumont, D.; Ellis, R. J.; Zorz, N.; Simonin, J.-P.; Berthon, L. Understanding the Synergistic Effect on Lanthanides(III) Solvent Extraction by Systems Combining a Malonamide and a Dialkyl Phosphoric Acid. *Hydrometallurgy*, **2017**, *169*, 542–551. https://doi.org/10.1016/j.hydromet.2017.02.012.

[76] Lumetta, G. J.; Sinkov, S. I.; Krause, J. A.; Sweet, L. E. Neodymium(III) Complexes of Dialkylphosphoric and Dialkylphosphonic Acids Relevant to Liquid–Liquid Extraction Systems. *Inorg. Chem.*, **2016**, *55* (4), 1633–1641. https://doi.org/10.1021/acs.inorgchem.5b02524.

[77] Campbell, E.; Holfeltz, V. E.; Hall, G. B.; Nash, K. L.; Lumetta, G. J.; Levitskaia, T. G. Extraction Behavior of Ln(III) Ions by T2EHDGA/n-Dodecane from Nitric Acid and Sodium Nitrate Solutions. *Solvent Extr. Ion Exch.*, **2018**, *36* (4), 331–346. https://doi.org/10.1080/07366299.2018.1447261.

[78] Rama Swami, K.; Kumaresan, R.; Nayak, P. K.; Venkatesan, K. A.; Antony, M. P. Extraction of Eu(III) in Diglycolamide-Organophosphorous Acid and the Interaction of Binary Solution with Eu(III) Studied by FTIR Spectroscopy. *Vib. Spectrosc.*, **2017**, *93*, 1–11. https://doi.org/10.1016/j.vibspec.2017.08.006.

[79] Gullekson, B. J.; Brown, M. A.; Paulenova, A.; Gelis, A. V. Speciation of Select F-Elements with Lipophilic Phosphorus Acids and Diglycol Amides in the ALSEP Backward-Extraction Regime. *Ind. Eng. Chem. Res.*, **2017**, *56* (42), 12174–12183. https://doi.org/10.1021/acs.iecr.7b02379.

[80] Tkac, P.; Vandegrift, G. F.; Lumetta, G. J.; Gelis, A. V. Study of the Interaction between HDEHP and CMPO and Its Effect on the Extraction of Selected Lanthanides. *Ind. Eng. Chem. Res.*, **2012**, *51* (31), 10433–10444. https://doi.org/10.1021/ie300326d.

[81] Ruikar, P. B.; Nagar, M. S.; Subramanian, M. S. Extraction of Uranium, Plutonium and Some Fission Products with γ-Irradiated Unsymmetrical and Branched Chain Dialkylamides. *J. Radioanal. Nucl. Chem.*, **1993**, *176* (2), 103–111. https://doi.org/10.1007/BF02163190.

[82] Ruikar, P. B.; Nagar, M. S.; Subramanian, M. S.; Gupta, K. K.; Varadarajan, N.; Singh, R. K. Extraction Behavior of Uranium(VI), Plutonium(IV) and Some Fission Products with Gamma Pre-Irradiatedn-Dodecane Solutions of N,N'-Dihexyl Substituted Amides. *J. Radioanal. Nucl. Chem.*, **1995**, *196* (1), 171–178. https://doi.org/10.1007/BF02036302.

[83] Mowafy, E. A. The Effect of Previous Gamma-Irradiation on the Extraction of U(VI), Th(IV), Zr(IV), Eu(III) and Am(III) by Various Amides. *J. Radioanal. Nucl. Chem.*, **2004**, *260* (1), 179–187. https://doi.org/10.1023/B:JRNC.0000027078.93004.a6.

[84] Drader, J.; Saint-Louis, G.; Muller, J. M.; Charbonnel, M.-C.; Guilbaud, P.; Berthon, L.; Roscioli-Johnson, K. M.; Zarzana, C. A.; Rae, C.; Groenewold, G. S.; et al. Radiation Chemistry of the Branched-Chain Monoamide Di-2-Ethylhexyl-Isobutyramide. *Solvent Extr. Ion Exch.*, **2017**, *35* (7), 480–495. https://doi.org/10.1080/07366299.2017.1379713.

[85] Condamines, N.; Musikas, C. THE EXTRACTION BY N, N-DIALKYLAMIDES.I. HNO3 AND OTHER INORGANIC ACIDS. *Solvent Extr. Ion Exch.*, **1988**, *6* (6), 1007–1034. https://doi.org/10.1080/07366298808917975.

[86] Déjugnat, C.; Berthon, L.; Dubois, V.; Meridiano, Y.; Dourdain, S.; Guillaumont, D.; Pellet-Rostaing, S.; Zemb, T. Liquid-Liquid Extraction of Acids and Water by a Malonamide: I-Anion Specific Effects on the Polar Core Microstructure of the Aggregated Malonamide. *Solvent Extr. Ion Exch.*, **2014**, *32* (6), 601–619. https://doi.org/10.1080/07366299.2014.940229.

[87] Peppard, D. F.; Ferraro, J. R. The Preparation and Infra-Red Absorption Spectra of Several Complexes of Bis-(2-Ethylhexyl)-Phosphoric Acid. *J. Inorg. Nucl. Chem.*, **1959**, *10* (3), 275–288. https://doi.org/10.1016/0022-1902(59)80121-4.

[88] Marie, C.; Hiscox, B.; Nash, K. L. Characterization of HDEHP-Lanthanide Complexes Formed in a Non-Polar Organic Phase Using 31P NMR and ESI-MS. *Dalton Trans.*, **2012**, *41* (3), 1054–1064. https://doi.org/10.1039/C1DT11534K.

[89] Shu Qiding; Khayambashi Afshin; Wang Xinpeng; Wang Xiaolong; Feng Lei; Wei Yuezhou. Effects of γ Irradiation on Bis(2-Ethylhexyl)Phosphoric Acid Supported by Macroporous Silica-Based Polymeric Resins. *Radiochim. Acta*, **2018**, *106* (3), 249. https://doi.org/10.1515/ract-2017-2758.

[90] Mincher, B. J.; Modolo, G.; Mezyk, S. P. Review Article: The Effects of Radiation Chemistry on Solvent Extraction 3: A Review of Actinide and Lanthanide Extraction. *Solvent Extr. Ion Exch.*, **2009**, *27* (5–6), 579–606. https://doi.org/10.1080/07366290903114098.

[91] Galán, H.; Núñez, A.; Espartero, A. G.; Sedano, R.; Durana, A.; de Mendoza, J. Radiolytic Stability of TODGA: Characterization of Degraded Samples under Different Experimental Conditions. *ATALANTE 2012 Int. Conf. Nucl. Chem. Sustain. Fuel Cycles*, **2012**, *7*, 195–201. https://doi.org/10.1016/j.proche.2012.10.033.

[92] Zsabka, P.; Van Hecke, K.; Wilden, A.; Modolo, G.; Hupert, M.; Jespers, V.; Voorspoels, S.; Verwerft, M.; Binnemans, K.; Cardinaels, T. Gamma Radiolysis of TODGA and CyMe4BTPhen in the Ionic Liquid Tri-n-Octylmethylammonium Nitrate. *Solvent Extr. Ion Exch.*, **2020**, *38* (2), 212–235. https://doi.org/10.1080/07366299.2019.1710918.

[93] Horne, G. P.; Wilden, A.; Mezyk, S. P.; Twight, L.; Hupert, M.; Stärk, A.; Verboom, W.; Mincher, B. J.; Modolo, G. Gamma Radiolysis of Hydrophilic Diglycolamide Ligands in Concentrated Aqueous Nitrate Solution. *Dalton Trans.*, **2019**, *48* (45), 17005–17013. https://doi.org/10.1039/C9DT03918J.

[94] Sánchez-García, I.; Galán, H.; Perlado, J. M.; Cobos, J. Stability Studies of GANEX System under Different Irradiation Conditions. *EPJ Nucl. Sci Technol*, **2019**, *5*. https://doi.org/10.1051/epjn/2019049.

[95] Wilden, A.; Mincher, B. J.; Mezyk, S. P.; Twight, L.; Rosciolo-Johnson, K. M.; Zarzana, C. A.; Case, M. E.; Hupert, M.; Stärk, A.; Modolo, G. Radiolytic and Hydrolytic Degradation of the Hydrophilic Diglycolamides. *Solvent Extr. Ion Exch.*, **2018**, *36* (4), 347–359. https://doi.org/10.1080/07366299.2018.1495384.

[96] Rajesh Bhikaji Gujar; Gunesh Bhalchandra Dhekane; Ajay Bhagwan Patil; Prasanta Kumar Mohapatra. Effect of Irradiation on Some Actinide and Fission Product Ions' Extraction Using Several Tetraalkyl Diglycolamides. *Radiochim. Acta*, **2015**, *103* (5), 335–344. https://doi.org/10.1515/ract-2014-2292.

[97] Mincher, B. J. The Effects of Radiation Chemistry on Radiochemistry: When Unpaired Electrons Defy Great Expectations. *J. Radioanal. Nucl. Chem.*, **2018**, *316* (2), 799–804. https://doi.org/10.1007/s10967-018-5728-1.

[98] Mincher, B. J.; Modolo, G.; Mezyk, S. P. Review Article: The Effects of Radiation Chemistry on Solvent Extraction 3: A Review of Actinide and Lanthanide Extraction. *Solvent Extr. Ion Exch.*, **2009**, *27* (5–6), 579–606. https://doi.org/10.1080/07366290903114098.

[99] TACHIMORI, S.; ITO, Y. Radiation Damage of Organic Extractant in Partitioning of High-Level Liquid Waste, (I). *J. Nucl. Sci. Technol.*, **1979**, *16* (1), 49–56. https://doi.org/10.1080/18811248.1979.9730869.

[100] Tachimori, S.; Krooss, B.; Nakamura, H. Effect of Radiolysis Products of Di-(2-Ethylhexyl)Phosphoric Acid upon the Extraction of Lanthanides. *J. Radioanal. Chem.*, **1978**, *43* (1), 53–63. https://doi.org/10.1007/BF02519440.

[101] LaVerne, J. A.; Chang, Z.; Araos, M. S. Heavy Ion Radiolysis of Organic Materials. *Int. Symp. Prospects Appl. Radiat.*, **2001**, *60* (4), 253–257. https://doi.org/10.1016/S0969-806X(00)00357-1.
[102] Wojnarovits, L.; LaVerne, J. A. Comparison of the Linear Energy Transfer Effect in the Radiolysis of Cyclopentane, Cyclohexane and Cyclooctane. *J. Radioanal. Nucl. Chem.*, **1998**, *232* (1), 19–22. https://doi.org/10.1007/BF02383705.
[103] Ladrielle, T.; Wanet, P.; Lemaire, D.; Aspers, D. J. Alpha and Gamma Induced Radiolysis of Tributylphosphate. *Radiochem. Radioanal. Lett.*, **1983**, *59* (5–6), 355–363.
[104] Groenewold, G. S.; Elias, G.; Mincher, B. J.; Mezyk, S. P.; LaVerne, J. A. Characterization of CMPO and Its Radiolysis Products by Direct Infusion ESI-MS. *Talanta*, **2012**, *99*, 909–917. https://doi.org/10.1016/j.talanta.2012.07.056.
[105] Colette, S.; Amekraz, B.; Madic, C.; Berthon, L.; Cote, G.; Moulin, C. Use of Electrospray Mass Spectrometry (ESI-MS) for the Study of Europium(III) Complexation with Bis(Dialkyltriazinyl)Pyridines and Its Implications in the Design of New Extracting Agents. *Inorg. Chem.*, **2002**, *41* (26), 7031–7041. https://doi.org/10.1021/ic025637t.
[106] Colette, S.; Amekraz, B.; Madic, C.; Berthon, L.; Cote, G.; Moulin, C. Trivalent Lanthanide Interactions with a Terdentate Bis(Dialkyltriazinyl)Pyridine Ligand Studied by Electrospray Ionization Mass Spectrometry. *Inorg. Chem.*, **2003**, *42* (7), 2215–2226. https://doi.org/10.1021/ic025894y.
[107] Crowe, M. C.; Kapoor, R. N.; Cervantes-Lee, F.; Párkányí, L.; Schulte, L.; Pannell, K. H.; Brodbelt, J. S. Investigating Bidentate and Tridentate Carbamoylmethylphosphine Oxide Ligand Interactions with Rare-Earth Elements Using Electrospray Ionization Quadrupole Ion Trap Mass Spectrometry. *Inorg. Chem.*, **2005**, *44* (18), 6415–6424. https://doi.org/10.1021/ic0503028.
[108] Moulin, C.; Amekraz, B.; Colette, S.; Doizi, D.; Jacopin, C.; Lamouroux, C.; Plancque, G. Electrospray Mass Spectrometry for Actinides and Lanthanide Speciation. *Proc. Rare Earths04 Nara Jpn.*, **2006**, *408–412*, 1242–1245. https://doi.org/10.1016/j.jallcom.2005.04.177.
[109] Retegan, T.; Berthon, L.; Ekberg, C.; Fermvik, A.; Skarnemark, G.; Zorz, N. Electrospray Ionization Mass Spectrometry Investigation of BTBP – Lanthanide(III) and Actinide(III) Complexes. *Solvent Extr. Ion Exch.*, **2009**, *27* (5–6), 663–682. https://doi.org/10.1080/07366290903113991.
[110] Antonio, M. R.; Chiarizia, R.; Gannaz, B.; Berthon, L.; Zorz, N.; Hill, C.; Cote, G. Aggregation in Solvent Extraction Systems Containing a Malonamide, a Dialkylphosphoric Acid and Their Mixtures. *Sep. Sci. Technol.*, **2008**, *43* (9–10), 2572–2605. https://doi.org/10.1080/01496390802121537.
[111] Muller, J.; Berthon, L.; Zorz, N.; Simonin, J.-P. Characterization of Lanthanide and Actinide Complexes in the DIAMEX-SANEX Process. **2010**.
[112] Berthon, L.; Zorz, N.; Gannaz, B.; Lagrave, S.; Retegan, T.; Fermvik, A.; Ekberg, C. Use of Electrospray Ionization Mass Spectrometry for the Characterization of Actinide Complexes in Solution. *IOP Conf. Ser. Mater. Sci. Eng.*, **2010**, *9*, 012059. https://doi.org/10.1088/1757-899x/9/1/012059.
[113] McDonald, L. W.; Campbell, J. A.; Vercouter, T.; Clark, S. B. Characterization of Actinides Complexed to Nuclear Fuel Constituents Using ESI-MS. *Anal. Chem.*, **2016**, *88* (5), 2614–2621. https://doi.org/10.1021/acs.analchem.5b03352.
[114] Beom, Y. H.; Hee, L. I.; Sil, M. H. Determination of Radiolysis Products in Zirconium Salt of Di-(2-Ethylhexyl) Phosphoric Acid by High Performance Liquid Chromatography/Mass Spectrometry. *J. Liq. Chromatogr. Relat. Technol.*, **2003**, *26* (15), 2593–2604. https://doi.org/10.1081/JLC-120023803.